

## Article

# *Synchrospora* gen. nov., a New Peronosporaceae Genus with Aerial Lifestyle from a Natural Cloud Forest in Panama

Thomas Jung <sup>1,2,\*</sup> , Yilmaz Balci <sup>3</sup> , Kirk D. Broders <sup>4,5</sup> , Ivan Milenković <sup>1,6</sup> , Josef Janoušek <sup>1</sup>,  
Tomáš Kudláček <sup>1</sup> , Biljana Đorđević <sup>1</sup> and Marilia Horta Jung <sup>1,2</sup> 

- <sup>1</sup> Phytophthora Research Centre, Faculty of Forestry and Wood Technology, Mendel University in Brno, 613 00 Brno, Czech Republic; ivan.milenkovic@mendelu.cz (I.M.); josef.janousek@mendelu.cz (J.J.); tomas.kudlacek@mendelu.cz (T.K.); biljana.dordevic@mendelu.cz (B.Đ.); marilia.jung@mendelu.cz (M.H.J.)
- <sup>2</sup> Phytophthora Research and Consultancy, 83131 Nußdorf, Germany
- <sup>3</sup> USDA-APHIS Plant Protection and Quarantine, 4700 River Road, Riverdale, MD 20737, USA; yilmaz.balci@usda.gov
- <sup>4</sup> Smithsonian Tropical Research Institute, Apartado Panamá, Panama City 0843-03092, Panama; kirk.broders@usda.gov
- <sup>5</sup> USDA, Agricultural Research Service, National Center for Agricultural Utilization Research, Mycotoxin Prevention and Applied Microbiology Research Unit, Peoria, IL 61604, USA
- <sup>6</sup> Faculty of Forestry, University of Belgrade, Kneza Višeslava 1, 11030 Belgrade, Serbia
- \* Correspondence: thomas.jung@mendelu.cz; Tel.: +420-545136172

**Abstract:** During a survey of *Phytophthora* diversity in Panama, fast-growing oomycete isolates were obtained from naturally fallen leaves of an unidentified tree species in a tropical cloud forest. Phylogenetic analyses of sequences from the nuclear ITS, LSU and *βtub* loci and the mitochondrial *cox1* and *cox2* genes revealed that they belong to a new species of a new genus, officially described here as *Synchrospora* gen. nov., which resided as a basal genus within the *Peronosporaceae*. The type species *S. medusiformis* has unique morphological characteristics. The sporangiophores show determinate growth, multifurcating at the end, forming a stunted, candelabra-like apex from which multiple (8 to >100) long, curved pedicels are growing simultaneously in a medusa-like way. The caducous papillate sporangia mature and are shed synchronously. The breeding system is homothallic, hence more inbreeding than outcrossing, with smooth-walled oogonia, plerotic oospores and paragynous antheridia. Optimum and maximum temperatures for growth are 22.5 and 25–27.5 °C, consistent with its natural cloud forest habitat. It is concluded that *S. medusiformis* as adapted to a lifestyle as a canopy-dwelling leaf pathogen in tropical cloud forests. More oomycete explorations in the canopies of tropical rainforests and cloud forests are needed to elucidate the diversity, host associations and ecological roles of oomycetes and, in particular, *S. medusiformis* and possibly other *Synchrospora* taxa in this as yet under-explored habitat.

**Keywords:** oomycete; evolution; phylogeny; caducity; synchronous sporulation; adaptation; homothallic; tropical; canopy; leaf pathogen



**Citation:** Jung, T.; Balci, Y.; Broders, K.D.; Milenković, I.; Janoušek, J.; Kudláček, T.; Đorđević, B.; Horta Jung, M. *Synchrospora* gen. nov., a New Peronosporaceae Genus with Aerial Lifestyle from a Natural Cloud Forest in Panama. *J. Fungi* **2023**, *9*, 517. <https://doi.org/10.3390/jof9050517>

Academic Editor: Lei Cai

Received: 14 March 2023

Revised: 20 April 2023

Accepted: 23 April 2023

Published: 27 April 2023



**Copyright:** © 2023 by the authors. Licensee MDPI, Basel, Switzerland. This article is an open access article distributed under the terms and conditions of the Creative Commons Attribution (CC BY) license (<https://creativecommons.org/licenses/by/4.0/>).

## 1. Introduction

The Peronosporaceae, a sister family of the Pythiaceae, belong to the Peronosporales, Peronosporomycetes, Stramenipila and currently comprise 25 genera, i.e., *Calycofera*, *Halophytophthora*, *Nothophytophthora*, *Phytophthora*, *Phytopythium* and 20 genera of downy mildews (DMs) [1–9]. Several phylogenetic studies have demonstrated that *Phytophthora* is monophyletic, with all DMs residing as two separate clades within *Phytophthora*, rendering *Phytophthora* paraphyletic with respect to its DM descendants [4,6–8,10–16]. Due to the monophyly and the biological and structural cohesion of *Phytophthora*, its historic and social impacts and its importance in scientific communication and biosecurity protocols, Brasier et al. [16] proposed to conserve the current nomenclatural status. They also argued

that paraphyletic jumps, such as the emergence of descendants with a new lifestyle (the DMs) from an ancestral and evolutionary successful, cohesive genus (*Phytophthora*), should be considered a normal feature of evolution. Unlike *Phytophthora*, the genus *Pythium* was, in multigene phylogenetic analyses, shown to be polyphyletic [10,12,17–19] and, consequently, divided into *Pythium sensu stricto* and four new genera, i.e., *Phytopythium* (syn. *Ovatisporangium*), *Elongisporangium*, *Globisporangium* and *Pilasporangium* [20–23]. Because of its phylogenetic relatedness and morphological similarity to *Phytophthora*, *Phytopythium* was assigned to the Peronosporaceae, whereas the other four genera constitute the Pythiaceae [4,6,9,22].

In 1952, Gäumann [24], based on morphological and pathogenic data, postulated an evolutionary development from the saprophytic *Pythium* species via hemibiotrophic or necrotrophic *Phytophthora* species to the obligate biotrophic downy mildews, which was confirmed later by various phylogenetic analyses. While *Calycofera*, *Halophytophthora* and *Phytopythium* species are mostly saprotrophs and/or necrotrophic opportunistic plant pathogens, most *Phytophthora* species have a hemibiotrophic or necrotrophic lifestyle as primary plant pathogens. In addition, predominantly aquatic *Phytophthora* species within phylogenetic clades 6, 9 and 10 have a partially saprotrophic lifestyle, and 46.7% of the 210 known culturable *Phytophthora* species are able to thrive as saprotrophs in water-bodies [5,9,16,25–34]. In contrast, all ca 900 DM species are highly specialised, obligate biotrophic plant pathogens [4,13,14,35]. The genera *Calycofera*, *Halophytophthora* and *Phytopythium* lack sporangial caducity congruent with their soilborne and/or aquatic lifestyle. In contrast, 75% of the eight described *Nothophytophthora* species, 26.7% of the 210 described *Phytophthora* species and all ca 900 DM species have caducous sporangia (or conidia), enabling an aerial or partially aerial lifestyle [4–6,9,13,14,16,22,31,34–36].

Since the 1960s, the number of devastating epidemics caused by introduced invasive *Phytophthora* species, including *P. austrocedrae*, *P. cinnamomi*, *P. lateralis*, *P. plurivora*, *P. ramorum*, *P. ×alni* or *P. ×cambivora* in both managed and natural ecosystems, has been increasing exponentially [16,26,37–71]. This has stimulated extensive *Phytophthora* surveys in previously unexplored natural ecosystems across most continents using classical baiting and isolation methods and sometimes metagenomic approaches as well. These surveys have unveiled an unprecedented diversity of described and previously unknown *Phytophthora* taxa in various ecological niches [6,16,30,31,41,44,45,47,72–94].

During a survey of *Phytophthora* diversity in Central America, fast-growing isolates that morphologically resemble the *Phytophthora* species were obtained from naturally fallen leaves in a tropical cloud forest in Panama. A preliminary phylogenetic analysis of ITS rDNA sequences suggested that they belong to a previously unknown distinct species from a potentially new Peronosporaceae genus. In this study, morphological and physiological characteristics were used in combination with DNA sequence data from three nuclear, i.e., ITS, part of the 28S large subunit (LSU) and  $\beta$ -tubulin, and the two mitochondrial *cox1* and *cox2* gene regions to characterise and officially describe the new oomycete genus as *Synchrospora* gen. nov. and the new taxon as *S. medusiformis* sp. nov.

## 2. Materials and Methods

### 2.1. Isolate Collection and Maintenance

Details of all isolates used in the phylogenetic, morphological and temperature–growth studies are given in Table 1 and Table S1. Sampling and isolation methods from naturally fallen necrotic leaves were according to [45]. For all isolates, single hyphal tip cultures were produced under the stereomicroscope from the margins of fresh cultures on V8–juice agar (V8A; 20 g agar, 3 g CaCO<sub>3</sub>, 100 mL Campbell’s V8 juice, 900 mL distilled water). Stock cultures were maintained on V8A and carrot agar (CA; 20 g agar, 3 g CaCO<sub>3</sub>, 200 g carrots, 1000 mL distilled water; [68]) at 20 °C in the dark. All isolates of the new genus *Synchrospora* were preserved in the culture collection maintained at the Phytophthora Research Centre, Mendel University, in Brno. The ex–type culture was deposited at the Westerdijk Fungal

Biodiversity Institute, Utrecht, Netherlands (Table 1), and the novel taxonomic description and nomenclature were submitted to MycoBank ([www.mycobank.org](http://www.mycobank.org)).

**Table 1.** Details of *Synchrospora* isolates used in the morphological and growth–temperature studies.

Species	Isolate Codes <sup>1</sup> ; Status <sup>2</sup>	Host/Habitat	Location; Year; Collectors
<i>Synchrospora medusifformis</i>	CBS 149011 = PA229; T	Fallen leaf, tropical cloud forest	Panama, Volcano Baru; 2019; K.D. Broders and Y. Balci
<i>S. medusifformis</i>	PA228	Fallen leaf, tropical cloud forest	Panama, Volcano Baru; 2019; K.D. Broders and Y. Balci
<i>S. medusifformis</i>	PA230	Fallen leaf, tropical cloud forest	Panama, Volcano Baru; 2019; K.D. Broders and Y. Balci
<i>S. medusifformis</i>	PA231	Fallen leaf, tropical cloud forest	Panama, Volcano Baru; 2019; K.D. Broders and Y. Balci
<i>S. medusifformis</i>	PA232	Fallen leaf, tropical cloud forest	Panama, Volcano Baru; 2019; K.D. Broders and Y. Balci

<sup>1</sup> Abbreviations of isolates and culture collections: CBS = CBS collection at the Westerdijk Fungal Biodiversity Institute, Utrecht, Netherlands; PA: Culture collection of Mendel University in Brno, Czech Republic. <sup>2</sup> T, ex-type strain.

## 2.2. DNA Extraction, Amplification and Sequencing

For all five *Synchrospora* isolates obtained in this study, 10 ex-type isolates from the genera *Halophytophthora* and *Nothophytophthora* and the neotype isolates of *P. infestans* and *P. ×cambivora* DNA were extracted from c. 15–100 mg of mycelium scraped from 1–3-wk-old V8A cultures, placed into 2 mL homogenisation tubes (Lysis Matrix A; MP Biomedicals, Irvine, USA) and disrupted using a Precellys Evolution instrument (Bertin Technologies, Montigny-le-Bretonneux, France) until the mixture was homogenous. DNA was purified using the Monarch Genomic DNA Purification Kit (New England Biolabs, Ipswich, USA) and treated with RNase A following the manufacturer’s protocol for tissue samples. DNA was eluted with 100 µL of pre-warmed elution buffer and preserved at –80 °C for long-term storage. Three nuclear gene regions, i.e., the internal transcribed spacer region (ITS1–5.8S–ITS2) of the ribosomal RNA gene (ITS), the 5’ terminal domain of the large subunit (28S-LSU) of the nuclear ribosomal RNA and β-tubulin (*βtub*), and the two mitochondrial genes cytochrome-c oxidase 1 (*cox1*) and 2 (*cox2*), were amplified and sequenced (Table 2). PCR amplifications were performed using a LightCycler 480 II instrument (Roche, Basel, Switzerland) or Eppendorf Mastercycler nexus GSX1 (Eppendorf, Hamburg, Germany). All primers were synthesised by Elizabeth Pharmacon spol. s.r.o. (Brno, Czech Republic). Their annealing temperatures were estimated using a Tm calculator (<http://tmcalsculator.neb.com/#!/main>, accessed on 24 February 2023) and adjusted empirically, according to observed PCR amplification rates. Table 2 provides a comprehensive overview of the PCR conditions and primers used. Primer FM35\_Oom2 was designed using a global alignment of *cox2* sequences from all described species of *Calycofera*, *Halophytophthora*, *Nothophytophthora*, *Phytophthora*, *Phytophythium* and selected species from other oomycete genera. Each nucleotide was carefully checked to identify whether it is conserved and, if necessary, replaced by a degenerate nucleotide. PCR products were visualised by gel electrophoresis (300 V; 5 min) using 2% agarose gel stained by DNA Stain G (SERVA, Heidelberg, Germany). All amplicons were purified and sequenced in both directions by Eurofins Genomics GmbH (Cologne and Ebersberg, Germany) using the amplification primers, except for the LSU amplicons, which required two additional primers (Table 2). Electropherograms were quality checked, and forward and reverse reads were compiled using Geneious Prime<sup>®</sup> v. 2022.0.2 (Biomatters Ltd., Auckland, New Zealand). Pronounced double peaks were considered as heterozygous positions and labelled according to the IUPAC (International Union of Pure and Applied Chemistry; <https://iupac.org>, accessed on 24 February 2023) coding system. All sequences generated in this study were deposited in GenBank, and accession numbers are given in Table S1.

### 2.3. Phylogenetic Analyses

The sequences obtained in this work were complemented with sequences deposited in GenBank. Sequences of all loci used in the analyses were aligned using the MAFFT v. 7 [95] plugin within the Geneious Prime<sup>®</sup> v. 2023.0.4 software (Biomatters Ltd., Auckland, New Zealand) by the E-INS-I strategy (ITS) or the G-INS-I strategy (all other loci).

To study the phylogenetic position of the potentially new genus among other oomycete genera, a five-partition (LSU-ITS-*βtub-cox1-cox2*) dataset of representative species from all genera of the Peronosporaceae and Pythiaceae together with five isolates from the new species were analysed with *Saprolegnia parasitica* (CBS 223.65) and *Aphanomyces euteiches* (ATCC 201684) as outgroups (dataset: 60 isolates and 4954 characters). Maximum likelihood (ML) and Bayesian (BI) analyses were carried out.

Within the ML analysis, each gene was treated as a separate partition, and best-fitting evolutionary models were estimated with PartitionFinder 2 [96] based on the corrected Akaike Information Criterion (AICc). The analysis was done for both linked and unlinked branch lengths, and the results were the same. The largest set of models possible was tested, including models with base frequencies estimated using maximum likelihood (84 models in total; option models = allx;). All possible partitioning schemes were analysed (option search = all;).

Phylogenetic inference estimated based on the ML method was produced in RAxML-NG 1.1.0 [97]. The necessary number of bootstrap replicates was determined automatically using the MRE-based bootstrapping test [98] with the default cut-off value 0.03 (option -bs-cutoff 0.03). The analysis converged before reaching the maximum number of replicates, which was set to 10,000 (option -autoMRE{10000}). As a support metric, we used Transfer Bootstrap Expectation [99]. As a summarising tree, the 50% majority rule consensus tree was created using SumTrees 4.4.0 within the Python library DendroPy 4.4.0 [100]. Edge lengths of the summarising tree were calculated as mean lengths for the corresponding edges in the input set of trees.

For the BI analysis, a Metropolis-coupled MCMC method (MC3) implemented in the CoupledMCMC package [101] with four chains (three heated and one cold) was used. The chain length was set to 20,000,000, and every 5000th state was sampled. Target switch probability was set to the recommended value of 0.234 [102,103]. Site models for individual genes were selected automatically by model averaging implemented in the bModelTest package [104]. The uncorrelated lognormal relaxed molecular clock model [105] was used. Substitutions per site were used as the unit of branch lengths of the sampled trees. Parameter estimates were summarised with TreeAnnotator 2.6.0 (part of BEAST 2) and mapped onto the 50% majority-rule consensus tree built with SumTrees 4.4.0 [100]. The option “force-rooted” was used, telling SumTrees to treat the tree as rooted. Edge lengths were calculated as mean lengths for the corresponding edges in the input set of trees. The posterior estimates of the parameters were summarised with Tracer 1.7.1 [106]. The quality of the parameter estimates was assessed based on visual analysis of trace plots and ESS values. Proper sampling was indicated by the minimum ESS value of 200 (standard approach). Likelihood and most of the other parameters of the final tree were higher than 200. Burn-in was set to 25%. Branches with a support value  $\leq 0.5$  were collapsed using TreeGraph 2 [107].

Phylogenetic trees were visualised in TreeGraph2 v. 2.15.0-887 beta [107] and/or MEGA 11 v. 11.0.11 [108] and edited in figure editor programs. The dataset and trees deriving from BI and ML analyses are available from the Dryad Digital Repository (<https://datadryad.org>; <https://doi.org/10.5061/dryad.p2ngf1vvt>).

**Table 2.** PCR conditions and details of primers used for amplification and sequencing of oomycete isolates.

Locus	Primer Names	Primer Sequences (5'-3')	Orientation	Annealing Temperature (°C); Extension Time (s)	Reference for Primer Sequences
<i>βtub</i> <sup>1,2</sup>	TUBUF2	CGGTAACAACCTGGGCCAAGG	Forward	68; 12	[12]
	TUBUR1	CCTGGTACTGCTGGTACTCAG	Reverse		
	Btub_F1A	GCCAAGTTCTGGGARGTSAT	Forward	66; 15	[109]
	Btub_R1A	CCTGGTACTGCTGGTAYTCMGA	Reverse		
<i>cox1</i>	OomCoxI-Levup	TCAWCWMGATGGCTTTTTTCAAC	Forward	60; 10	[110]
	<sup>1</sup> OomCoxI-Levlo	CYTCHGGRTGWCCRAAAAACCAAA	Reverse		
	COXF4N <sup>3</sup>	GTATTTCTTCTTTATTAGGTGC	Forward	50; 65	[12]
	COXR4N <sup>3</sup>	CGTGAACATAATGTTACATATAC	Reverse		
<i>cox2</i>	FM35 <sup>1,4</sup>	CAGAACCTTGGCAATTAGG	Forward	60; 20	[110,111]
	OomCoxI-Levlo	CYTCHGGRTGWCCRAAAAACCAAA	Reverse		
	FM35_Oom2 <sup>3,4</sup>	SCNKWACCTTGGCAAWTRGG	Forward	50; 80	[this study] [110]
	OomCoxI-Levlo	CYTCHGGRTGWCCRAAAAACCAAA	Reverse		
<i>cox1</i> and <i>cox2</i> <sup>3,4</sup>	FM35	CAGAACCTTGGCAATTAGG	Forward	50; 150	[12,31,110–113]
	COXR4N	CGTGAACATAATGTTACATATAC	Reverse		
	OomCoxI-Levlo <sup>5</sup>	CYTCHGGRTGWCCRAAAAACCAAA	Reverse		
	FM83_Oom <sup>5</sup>	CHCCNATAAARAATAACCARAARTG	Reverse		
	FM80_RC <sup>5</sup>	TTTCAACAAATCATAAAGATAT	Forward		
COX2-R <sup>5</sup>	CCATGATTAATACCACAAATTTCACTAC	Reverse			
ITS <sup>1</sup>	ITS1	TCCGTAGGTGAACCTGCGG	Forward	63–65; 12	[10,114]
	ITS4 <sup>6</sup>	TCCTCCGCTTATTGATATGC	Reverse		
	ITS6 <sup>6</sup>	GAAGGTGAAGTCGTAACAAGG	Forward		
LSU <sup>1,7</sup>	CTB6	GCATATCAATAAGCGGAGG	Forward	53; 20	[115,116]
	LR3 <sup>5</sup>	CCGTGTTTCAAGACGGG	Reverse		
	LR3R <sup>5</sup>	GTCTTGAAACACGGACC	Forward		
	LR7	TACTACCACCAAGATCT	Reverse		

<sup>1</sup> PCR protocol 1: 20 µL volume containing 10.4 µL H<sub>2</sub>O, 4 µL Q5 Reaction Buffer (5X), 1 µL of each primer (10 µM), 0.4 µL deoxynucleotide (dNTP) mixture (Meridian Bioscience, Memphis, USA) (2.5 mM each), 0.2 µL of Q5 High-Fidelity DNA Polymerase (2 U/µL) (New England Biolabs, Ipswich, USA), and 3 µL of gDNA. Initial denaturation for 30 s at 98 °C; 35 cycles consisting of 5 s at 98 °C, 20 s at optimised annealing temperature for each primer set, optimised length of extension at 72 °C; 2 min at 72 °C for final extension. <sup>2</sup> Two primer pairs were used separately: TUBUF2/TUBUR1 or Btub\_F1A/Btub\_R1A. <sup>3</sup> PCR protocol 2: 20 µL volume containing 10 µL H<sub>2</sub>O, 4 µL PrimeSTAR GXL Buffer (5X), 0.8 µL of each primer, 1.6 µL dNTP mixture, 0.4 µL PrimeSTAR GXL DNA Polymerase (1.25 U/µL) (TaKaRa Bio, Kusatsu, Shiga, Japan), and 3 µL of gDNA. Initial denaturation for 5 s at 98 °C; 35 cycles consisting of 10 s at 98 °C, 15 s at optimised annealing temperature, optimised length of extension at 68 °C; 5 min at 68 °C for final extension. <sup>4</sup> Three different primer pairs were used separately for COX II amplification: FM35/OomCoxI-Levlo or FM35\_Oom2/OomCoxI-Levlo or FM35\_Oom2/COX4RN (in this case also COX I was amplified too). <sup>5</sup> Primers used exclusively for sequencing. <sup>6</sup> Two primer combinations were used separately: ITS1/ITS4 or ITS6/ITS4. <sup>7</sup> Double concentration of Q5 polymerase.

#### 2.4. Morphology of Asexual and Sexual Structures

Formation of sporangia was induced by submersing two 12–15 mm square discs cut from the growing edge of a 2–4-d-old V8A colony in a 90-mm-diameter Petri dish in non-sterile soil extract (50 g of oak forest soil in 1 000 mL of distilled water, filtered after 24 h) [39]. The Petri dishes were incubated at 20 °C, and natural daylight and the soil extract changed after ca 6 h [74]. Shape, type of apex, caducity, pedicels and special features of sporangia were recorded after 24–48 h. For each isolate, 50 sporangia were measured at ×400 using a compound microscope (Zeiss Imager.Z2), a digital camera (Zeiss Axiocam ICc3) and biometric software (Zeiss ZEN).

The formation of gametangia (oogonia and antheridia) and their characteristic features were examined after 21–30 d growth at 20 °C in the dark on V8A. For each isolate, 50 oogonia, oospores and antheridia chosen at random were measured under a compound microscope at ×400. The oospore wall index was calculated according to [117].

#### 2.5. Colony Morphology, Growth Rates and Cardinal Temperatures

Colony growth patterns of all five isolates of *S. medusiformis* were described from 7-d-old cultures grown at 20 °C in the dark in 90-mm plates on CA, V8A and potato–dextrose agar (PDA; HiMedia, Mumbai, India) according to patterns observed previously [9,31,61].

For temperature–growth relationships, all five isolates of *S. medusiformis* were sub-cultured onto 90 mm V8A plates and incubated for 24 h at 20 °C to stimulate onset of growth [118]. Then, three replicate plates per isolate were transferred to 5, 10, 15, 20, 22.5, 25, 27.5, 30, 32.5 and 35 °C. Radial growth was recorded after 4–10 days, before colonies reached the margin of the Petri dishes, along two lines intersecting the centre of the inoculum at right angles, and the mean growth rates (mm/d) were calculated. To determine the lethal temperature, plates showing no growth at 27.5, 30, 32.5 or 35 °C were returned to 20 °C.

### 3. Results

#### 3.1. Phylogeny

Both the BI and the ML analyses of the 5-partition (LSU–ITS–*βtub*–*cox1*–*cox2*) dataset (4954 characters) produced phylogenetic trees with full support for both the deeper and end nodes and almost identical topology. The Bayesian tree is presented here with both Bayesian Posterior Probability values and Maximum Likelihood bootstrap values included (Figure 1, Dryad Dataset, <https://doi.org/10.5061/dryad.p2ngf1vvt>). The five known Peronosporaceae genera, *Calycofera*, *Phytophythium*, *Halophytophthora*, *Nothophytophthora* and *Phytophthora*, were well differentiated with full support, as were the Pythiaceae genera *Elongisporangium*, *Globisporangium*, *Pilasporangium* and *Pythium* (Figure 1). The mostly terrestrial soil-, air- and waterborne genera *Phytophthora* and *Nothophytophthora* constituted sister genera with the predominantly marine genus *Halophytophthora* residing in a basal position to them. “*Halophytophthora*” *exoprolifera* belonged to an undescribed distinct genus basal to the *Halophytophthora*–*Nothophytophthora*–*Phytophthora* cluster, while the cluster comprising the sister genera *Calycofera* and *Phytophythium* resided in a basal position to the other known Peronosporaceae genera, confirming recently published phylogenies [6,9,36]. The five isolates of the new species *Synchrospora medusiformis* formed a fully supported distinct clade that resided in a basal position to the cluster comprising the described Peronosporaceae genera, suggesting *Synchrospora* as the basal genus of the Peronosporaceae.

Across a 5-partition (LSU–ITS–*βtub*–*cox1*–*cox2*) alignment (4209 characters), *S. medusiformis* showed pairwise differences from its closest relative *Pilasporangium apinafurcum* at 614 positions, equivalent to a genetic distance of 14.6%. With 204 polymorphisms and 103 indels across a 788 bp alignment, differences were considerably higher (39.0%) in the ITS region with its non-coding parts than in the coding genes LSU (1260 bp; 86 polymorphic sites; 6.8% difference); *βtub* (918 bp; 99 polymorphisms and 6 indels; 11.4%); *cox1* (680 bp; 64 polymorphisms; 9.4%); and *cox2* (563 bp; 52 polymorphisms; 9.2%).

#### 3.2. Taxonomy

*Synchrospora* T. Jung, Y. Balci, K. Broders and M. Horta Jung, gen. nov. MycoBank MB 847829.

Etymology. Name refers to the synchronous production of numerous sporangia from one sporangiophore apex.

Type species. *Synchrospora medusiformis*.

In the only known species, *Synchrospora medusiformis*, sporangiophores are usually unbranched or infrequently have a short lateral branch, showing determinate growth multifurcating at the end in a subdichotomous way, forming a stunted, candelabra-like apex from which multiple (8 to >100) long arch- or hook-like curved pedicels grow and form the sporangia in a synchronous way, resulting in a multi-sporangia structure with a medusa-like appearance. Sporangia are narrow and elongated, mostly cylindrical to allantoid, usually with an asymmetric base and a papillate apex when mature, and caducous. After shedding, the pedicels usually become twisted. Sporangia germinate directly with multiple hyphae or indirectly by releasing 2–5 biflagellate zoospores through a very narrow exit pore without a discharge tube. No internal sporangial proliferation was observed. Very rarely, external proliferation of the sporangiophore occurs some distance from the apex. Chlamydospores are not formed. The breeding system is homothallic and,

hence, predominantly inbreeding, forming smooth-walled oogonia, containing plerotic thick-walled oospores with a large lipid globule, and paragynous antheridia. Hyphae often show undulating growth. Phylogenetically, *Synchrospora* belongs to the Peronosporaceae within the Peronosporales.

*Synchrospora medusiformis* T. Jung, Y. Balci, K. Broders and I. Milenković, sp. nov. (Figures 2–5). MycoBank MB 847831.

**Etymology:** The name refers to the medusa-like appearance of the sporangiophore apex with multiple sporangia on long arch-like pedicels.

**Holotype:** Panama, Province Chiriqui, Volcano Barú, isolated from a naturally fallen leaf of an unidentified tree species in a tropical cloud forest at an altitude of 2393 m. Collected: K. Broders and Y. Balci, November 2019; CBS H-24948 (holotype, dried culture on V8A, Herbarium CBS–KNAW Fungal Biodiversity Centre), CBS 149011 = PA229 (ex-type culture). ITS, *βtub*, LSU, *cox1* and *cox2* sequences GenBank accession nos. OQ600177, OQ605385, OQ600184, OQ605396 and OQ605417, respectively.

**Description:** Sporangiophores were not observed in solid agar but were produced abundantly in non-sterile soil extract. They were usually unbranched or infrequently formed short lateral hyphae. Sporangiophores showed determinate growth and were always multifurcating at the end, forming a stunted, candelabra-like apex from which multiple (8 to >100) pedicels were growing simultaneously (Figures 2 and 3). All sporangia at the end of the fully elongated pedicels from a sporangiophore apex were formed in a synchronous way, giving the mature multi-sporangia structure a medusa-like appearance (Figure 4). Sporangia were elongated, mostly cylindrical to allantoid (Figures 4 and 5A–G) or very rarely limoniform (Figure 5h), usually with an asymmetric curved base and a papillate apex when mature (Figures 4E,F and 5A–E). Sporangial dimensions of five isolates of *S. medusiformis* averaged  $22.3 \pm 2.6 \times 7.2 \pm 0.7 \mu\text{m}$  (overall range  $15.8\text{--}31.6 \times 5.5\text{--}9.2 \mu\text{m}$ ), with a range of isolate means of  $21.0\text{--}23.0 \times 7.1\text{--}7.4 \mu\text{m}$  and a length/breadth ratio of  $3.1 \pm 0.4$  (range of isolate means 2.96–3.21). Pedicels were arch-like or hook-like curved when still attached to the sporangiophore apex (Figures 3 and 4). Pedicel length was  $58.0 \pm 9.6 \mu\text{m}$  (overall range  $35.3\text{--}89.7 \mu\text{m}$ ; range of isolate means  $53.2\text{--}61.7 \mu\text{m}$ ). All sporangia arising from a sporangiophore apex were caducous and shed more or less synchronously (Figure 5A–E). After shedding, the pedicels often became twisted (Figure 5A–E). Sporangia germinated directly with multiple hyphae (Figure 5E) or indirectly by releasing two to three (in rare cases up to five) zoospores through a very narrow exit pore ( $1.6 \pm 0.2 \mu\text{m}$ ) without a discharge tube (Figure 5F–H). Zoospores were heterokont biflagellate with one longer flagellum and one shorter flagellum and limoniform to reniform whilst motile (Figure 5I–K), becoming spherical (av. diam =  $8.5 \pm 1.1 \mu\text{m}$ ) on encystment. No internal sporangial proliferation occurred. Very rarely, branching of the sporangiophore some distance from the apex was observed (Figure 4C).

All five isolates of *S. medusiformis* were homothallic. Gametangia were produced in single culture in V8A within 10–14 d. Oogonia were borne terminally or laterally, had smooth walls and thin stalks and were globose with round, non-tapering bases (Figure 6A–R). The mean diameter of oogonia was  $27.6 \pm 2.9 \mu\text{m}$  (overall range  $16.7\text{--}45.0 \mu\text{m}$  and range of isolate means  $25.6\text{--}29.9 \mu\text{m}$ ). They were exclusively plerotic, filling the oogonia completely and making a distinction between the oogonium and oospore walls in most cases impossible (Figure 6A–R). The oospores were globose with large lipid globules (=ooplasts), turning golden-brown during maturation (Figure 6A–R), and had a diameter of  $26.0 \pm 2.9 \mu\text{m}$  (overall range  $15.1\text{--}38.8 \mu\text{m}$ ), a wall diameter of  $1.44 \pm 0.19 \mu\text{m}$  (range  $0.87\text{--}2.37 \mu\text{m}$ ) and an oospore wall index of  $0.30 \pm 0.03$ . Oospore abortion was low (12.6% after 4 weeks). The antheridia were exclusively paragynous, club-shaped to subglobose, cylindrical or irregular (Figure 6A–R) and averaged  $10.8 \pm 2.4 \times 6.1 \pm 1.5 \mu\text{m}$ .

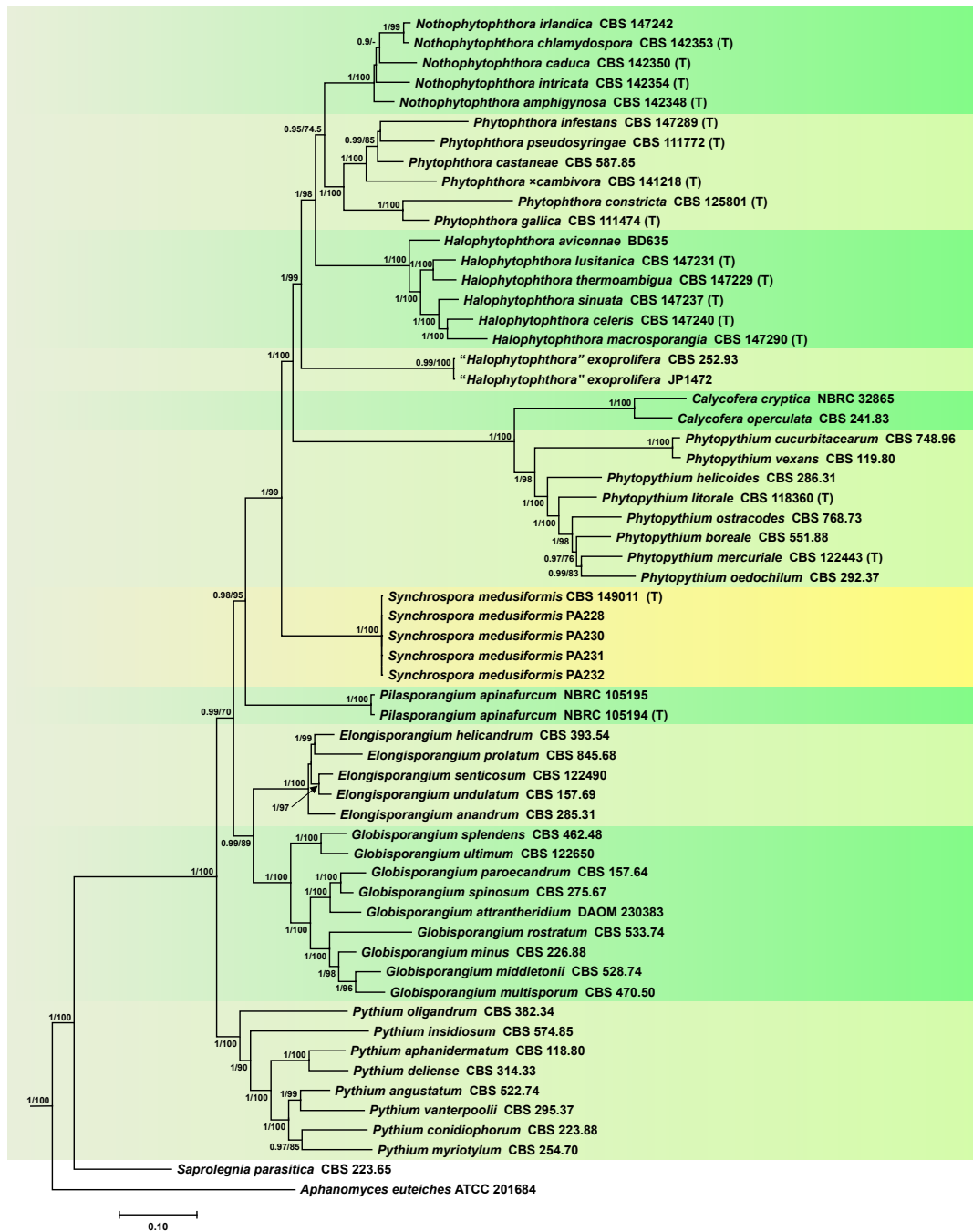


**Figure 1.** Fifty percent majority rule consensus phylogram derived from Bayesian phylogenetic analysis of a concatenated five-loci (LSU, ITS, *βtub*, *cox1*, *cox2*) dataset of *Synchrospora* gen. nov. and representative species from other genera of the Peronosporaceae and Pythiaceae. Bayesian posterior probabilities and maximum likelihood bootstrap values (in %) are indicated but not shown below 0.9 and 70%, respectively. *Saprolegnia parasitica* and *Aphanomyces euteiches* were used as outgroup taxa. Scale bar indicates 0.1 expected changes per site per branch.



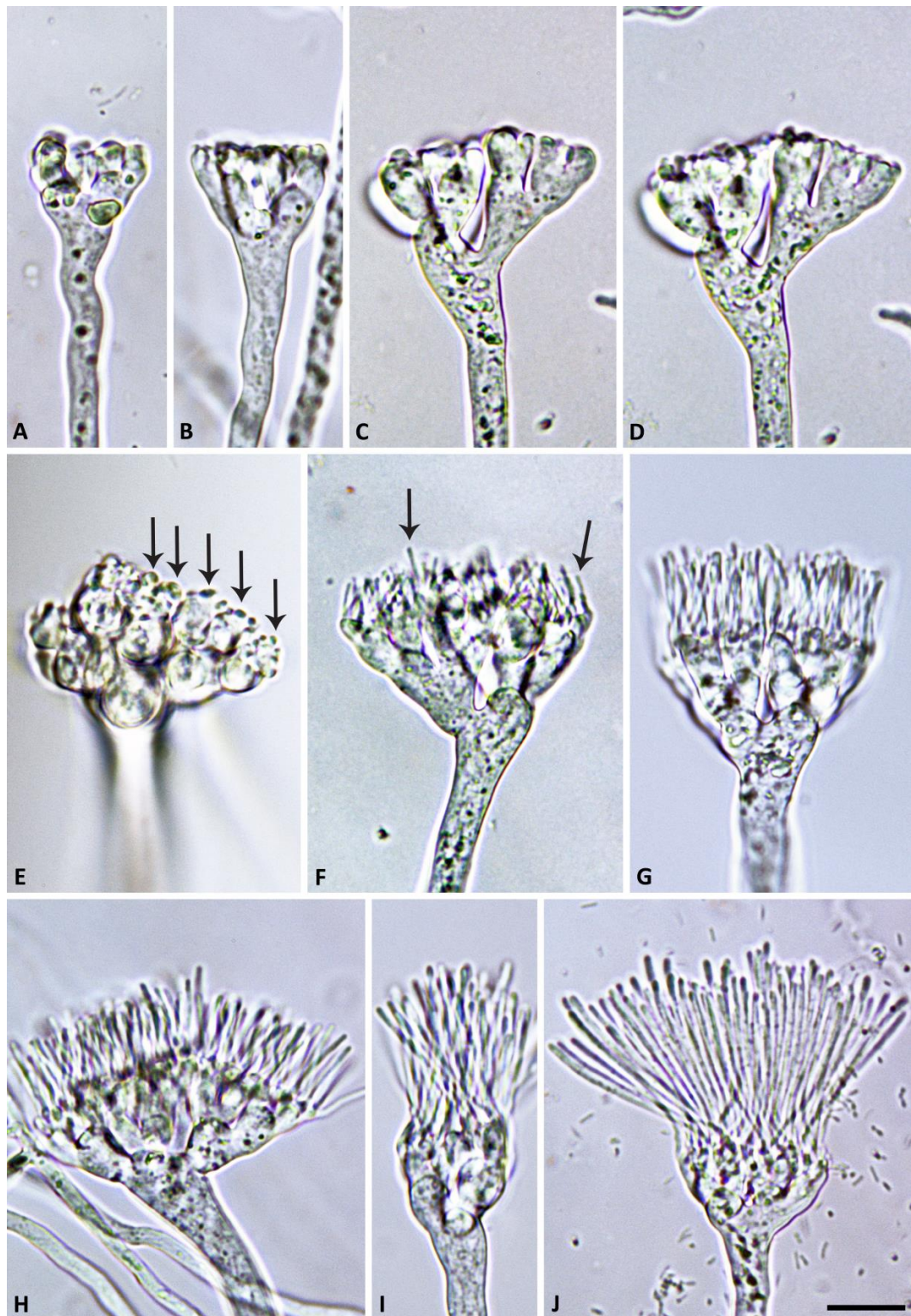


**Figure 2.** Morphological structures of *Synchronospora medusiformis* formed on V8 agar flooded with soil extract. (A–D) Candelabra-like branching of sporangiophore apices; (E,F) beginning growth of sporangial pedicels (arrows) from sporangiophore apices; (G–J) progressive growth of initially straight sporangial pedicels from sporangiophore apices. Scale bar: 15  $\mu\text{m}$ .



**Figure 3.** Morphological structures of *Synchrospora medusiformis* formed on V8 agar flooded with soil extract. (A,B) progressive growth of initially straight sporangial pedicels from sporangiophore apices; (C–G) progressive growth of increasingly curved, arch-like sporangial pedicels from sporangiophore apices. Scale bar: 25  $\mu$ m.

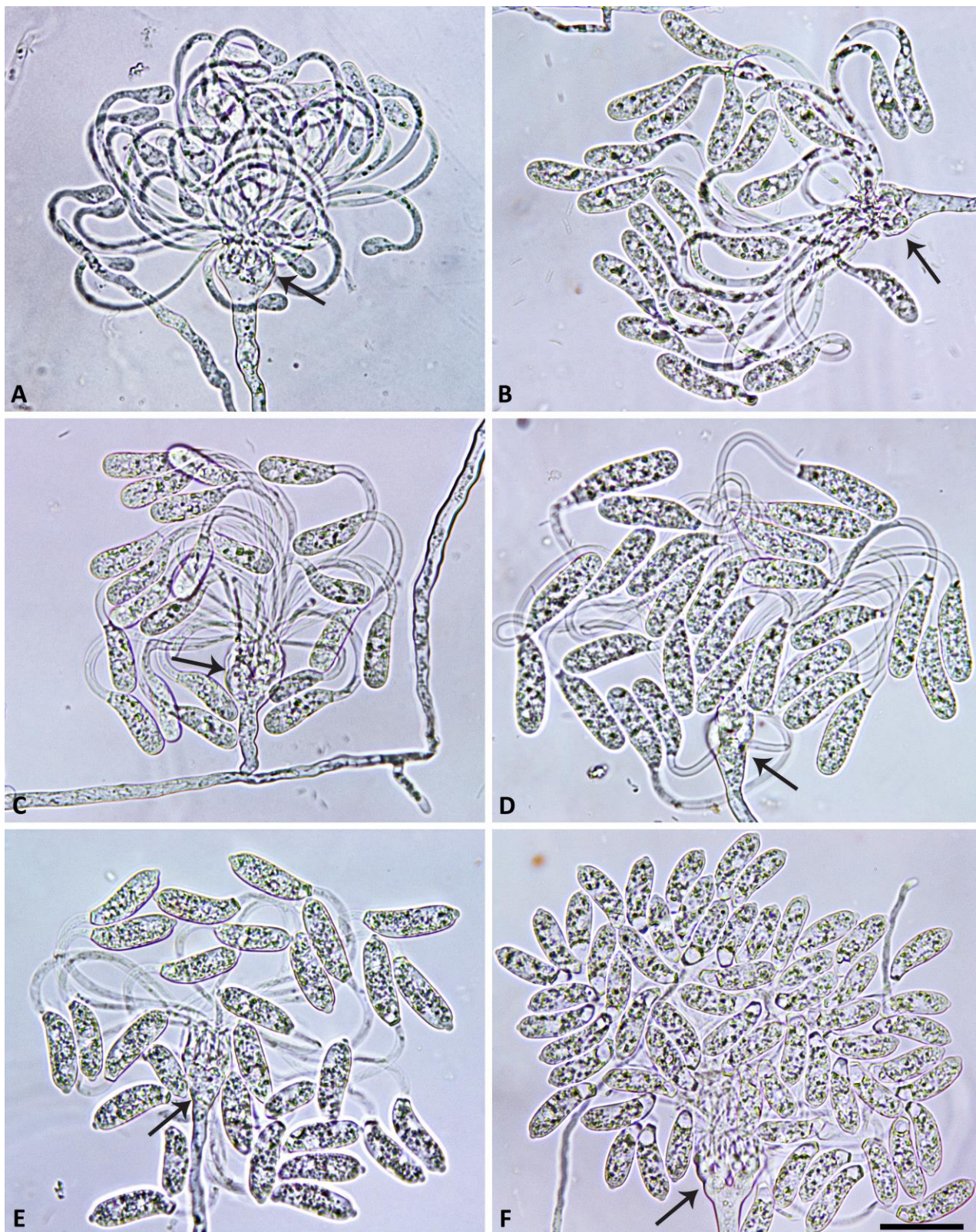


**Figure 4.** Morphological structures of *Synchrospora medusiformis* formed on V8 agar flooded with soil extract. (A–F) Medusa-like appearance of sporangiophore apices (arrows) with numerous long arch- or hook-like pedicels; (A–D) progressive formation of initially non-papillate sporangia at the ends of unbranched pedicels; (E,F) mature, papillate allantoid to tubular sporangia. Scale bar: 25  $\mu\text{m}$ .



**Figure 5.** Morphological structures of *Synchronospora medusiformis* formed on V8 agar flooded with soil extract. (A–E) Mature, papillate, allantoid sporangia; (A–D) caducous with mostly curved or twisted long pedicels; (E) beginning direct germination (arrows); (F,G) allantoid sporangia releasing zoospores; (H) empty limoniform sporangium after zoospore release; (I–K) motile heterokont zoospores with each two flagella of unequal length (arrows). Scale bar: 25  $\mu$ m.

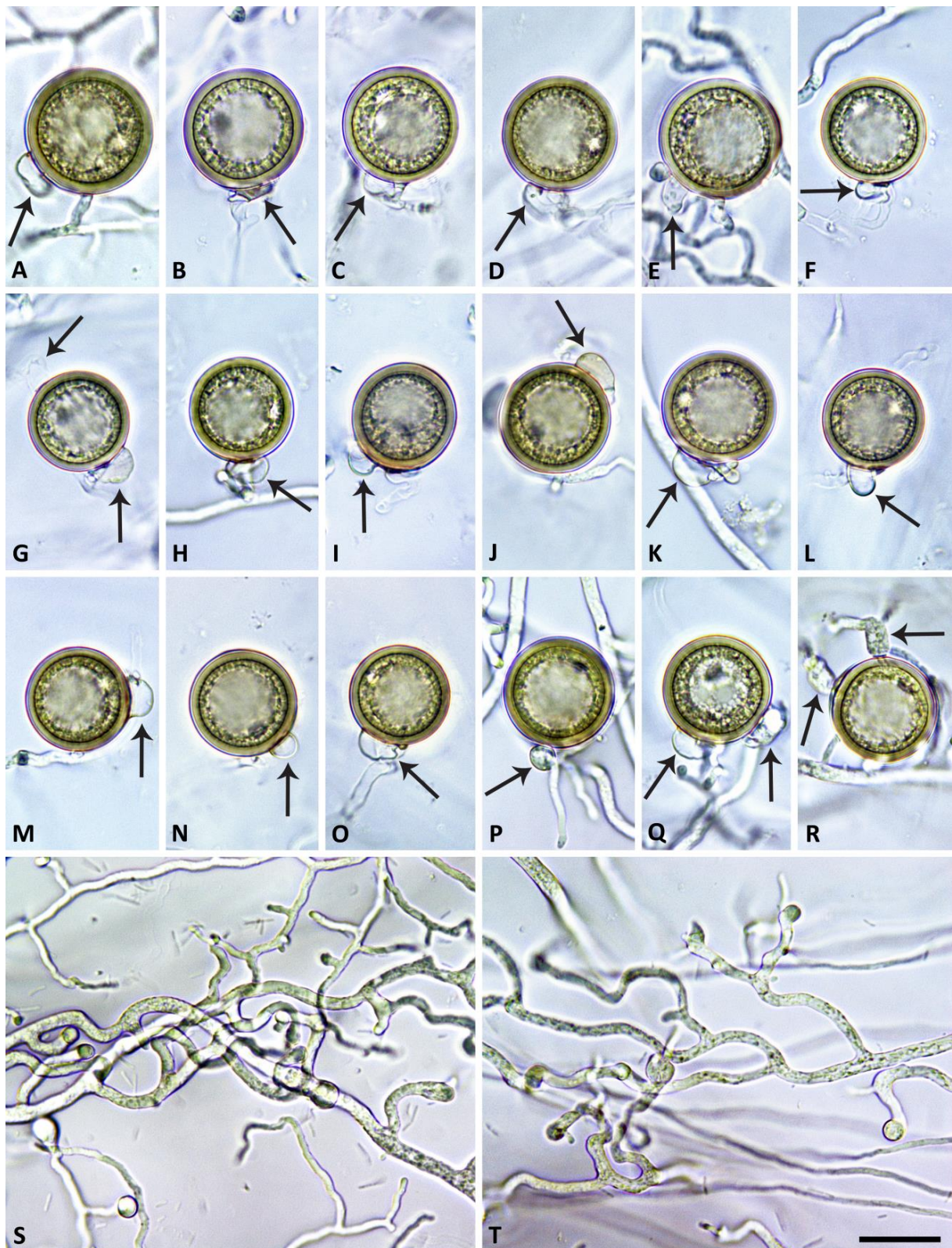


**Figure 6.** Morphological structures of *Synchrospora medusiformis* formed in solid V8 agar. (A–R) Mature, golden-brown, smooth-walled globose oogonia formed in single culture on very thin stalks, containing thick-walled fully plerotic oospores with large lipid globules (ooplasts), with one or sometimes two paragynous antheridia (arrows); (S,T) undulating hyphae without basal constrictions. Scale bar: 25  $\mu$ m.

Hyphae often showed undulating growth (Figure 6S,T).

Colony morphology, growth rates and cardinal temperatures: Colonies of *S. medusiformis* on V8A and CA were largely submerged with limited aerial mycelium, with a petaloid pattern on V8A and a chrysanthemum pattern on CA. On PDA, colonies were densely felty with petaloid to stoloniferous patterns (Figure 7). Temperature–growth relations on V8A are shown in Figure 8. All five isolates included in the growth test had similar growth rates and cardinal temperatures. The maximum growth temperature was between 25 and 27.5 °C. The ex-type isolate (CBS 149011) did not resume growth when plates incubated for 7 d at 27.5 °C were transferred to 20 °C. The other four isolates did not resume growth when plates incubated for 7 d at 30 °C were transferred to 20 °C. The average radial growth rate on V8A at the optimum temperature of 22.5 °C was  $12.5 \pm 0.58$  mm/d (isolate range 11.5–13.0 mm/d; Figure 8).

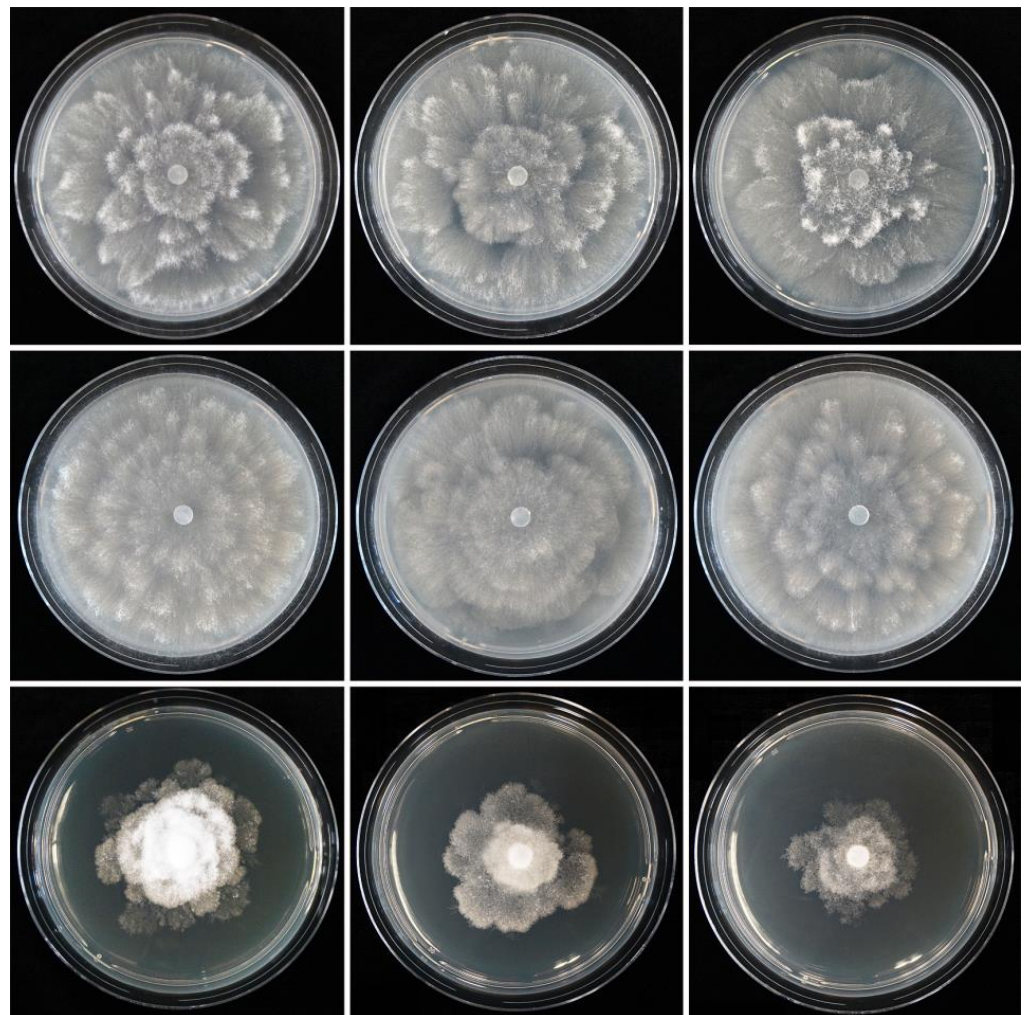


**Figure 7.** Colony morphology of *Synchrospora medusiformis* isolates CBS 149011, PA230 and PA231 (from left to right) after 7 d growth at 20 °C on V8 agar, carrot agar, potato–dextrose agar and malt extract agar (from top to bottom).

Other specimens examined (paratypes): Panama, Province Chiriqui, Volcán Barú, isolated from naturally fallen leaves of unidentified tree species in a tropical cloud forest at an altitude of 2393 m. Collected: K. Broders and Y. Balci, November 2019; PA228, PA230, PA231, PA232.

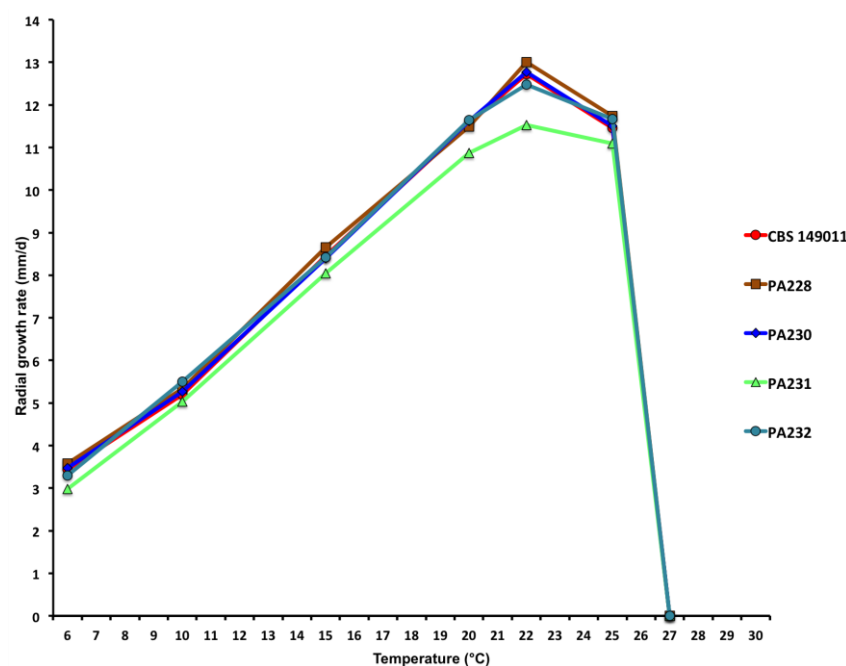


**Figure 8.** Mean radial growth rates of five isolates of *Synchrospora medusiformis* on V8 agar at different temperatures.

Notes: The only known species of the new genus *Synchrospora*, *S. medusiformis*, is differentiated from all other known oomycete species by its unique synchronous production of numerous (up to >100) caducous, long-pedicellate sporangia per multifurcating candelabra-like apex of sporangiophores with determinate growth enabling simultaneous aerial spread. In contrast, all aerial species of *Phytophthora* and *Nothophytophthora* produce sporangia individually on unbranched sporangiophores or consecutively on indeterminate sporangiophores, forming lax simple sympodia or dense compound sympodia [6,8,16,26,31,34,36]. Furthermore, the sporangia of *S. medusiformis* were, on average, smaller than in any known *Phytophthora* and *Nothophytophthora* species. Like *S. medusiformis*, all but two of the 20 known downy mildew (DM) genera also show determinate sporangiophore growth (*Viennotia* being the exception) and simultaneously ripening sporangia (*Sclerophthora* being the exception) [119]. Moreover, in several DM genera, the determinate sporangiophores also have dilated apices on which multiple sporangia or conidia are produced. These apices are saucer-shaped in *Bremia*, club-shaped in *Eraphthora*, cone- to club-shaped in *Basidiophora* and broad club-shaped to cylindrical in *Baobabopsis* [120–123]. However, none of the known DM genera form multifurcated candelabra-like sporangiophore apices. In addition, the pedicels of *S. medusiformis* are much longer than in any known DM species, and none of the known DM genera produce up to 100 or more sporangia per apex. Finally, the DMs are phylogenetically distant from *Synchrospora*, residing as two distinct clades within the paraphyletic genus *Phytophthora* [7,8,16], and are obligate biotrophic, nonculturable pathogens, whereas *S. medusiformis* grows well on various culture media.

#### 4. Discussion

During a survey of oomycete diversity in natural forests of Central America, fast growing oomycete isolates were obtained alongside a diverse community of known and new *Phytophthora*, *Phytophythium* and *Pythium* species (Y. Balci, K. Broders and T. Jung, unpublished results), from naturally fallen tree leaves collected in a tropical cloud forest near the peak of Volcano Barú in Panama. Phylogenetic analyses of a five-partition dataset of sequences from the nuclear ITS, LSU and *βtub* genes and the mitochondrial *cox1* and *cox2* genes placed them into a distinct, previously unknown species belonging to a new genus described here as *Synchrospora* gen. nov. Based on its distinct phylogenetic position and

unique set of morphological and physiological characteristics, the novel taxon is described here as *S. medusiformis*.

The multigene phylogenetic analysis demonstrated that *Synchrospora* resides in a basal position to a large cluster comprising all known Peronosporaceae genera, i.e., *Calycofera*, *Halophytophthora*, *Nothophytophthora*, *Phytophthora* (including the DMs) and *Phytophythium* [1,2,4,6,8,9,124]. Due to the phylogenetic position and the sporangial caducity of *S. medusiformis*, a common characteristic in the Peronosporaceae genera *Nothophytophthora* and *Phytophthora* including the DMs that has never been observed in any of the known Pythiaceae genera, *Synchrospora* is assigned to the Peronosporaceae constituting the basal genus of the family.

Despite the high number of oomycete surveys performed during the previous two decades in both managed and natural ecosystems across most continents, there is only one GenBank entry matching *Synchrospora* (ITS accession no. KM265501, 100% identical to *S. medusiformis*), which came from isolate E14413A (designated as Fungal sp. E14413A), obtained from stem tissue of the shrub species *Croton alnifolius* (Euphorbiaceae) during a fungal endophyte survey in a tropical cloud forest of Ecuador. This finding and the fact that all isolates of *S. medusiformis* examined in the present study originate from naturally fallen tree leaves in a remote tropical cloud forest near the peak of Volcano Barú in Panama suggest that this species is a neotropical canopy dweller in permanently humid cloud forests with a highly specialised aerial lifestyle as a leaf and bark pathogen.

Functionally, the synchronous production and ripening of up to more than 100 caducous sporangia per candelabra-like sporangiophore apex in *S. medusiformis* resembles 19 of the 20 DM genera [4,119,120,123,125–127], allowing simultaneous aerial spread with high inoculum pressure. Another similarity between *Synchrospora* and the DMs is the small size (and hence weight) of the sporangia increasing their aerial dispersibility, whereas the unusually long, curved and twisted pedicels most likely facilitate sporangial clustering and adherence to plant surfaces as recently suggested for aerial long-pedicellate *Phytophthora* species [16].

*Synchrospora medusiformis*, 75% of the eight described *Nothophytophthora* species, 26.7% of the 210 described *Phytophthora* species and all ca 900 DM species have caducous sporangia (or conidia) connected to an aerial or partially aerial lifestyle [4,6,13,14,16,31,34,36,123], whereas the other Peronosporaceae genera *Calycofera*, *Halophytophthora* and *Phytophythium* completely lack sporangial caducity [5,9,22,33]. Significant differences in sporangiophore growth and sporangial caducity between *Synchrospora* (determinate sporangiophores, synchronous production of up to >100 pedicellate caducous sporangia per candelabra-like sporangiophore apex); *Nothophytophthora* (indeterminate sporangiophores forming sympodia of non-pedicellate sporangia that mature non-synchronously; caducity by breaking off below a conspicuous opaque plug); *Phytophthora* (indeterminate sporangiophores forming sympodia of pedicellate sporangia that mature non-synchronously; caducity in airborne species); *Viennotia* (indeterminate sporangiophores, non-pedicellate caducous sporangia that mature non-synchronously); and the other 19 DM genera (determinate sporangiophores forming non-pedicellate or rarely pedicellate (cf. *Basidiophora*; [120]) caducous sporangia or conidia that mature synchronously) [3,4,6,16,26,34,36,119,123] suggest that sporangial caducity and an aerial or partially aerial lifestyle evolved independently in different Peronosporaceae genera in a convergent way.

During the past three decades, diversity of oomycete species and their ecological and pathogenic roles in soils and waterbodies of natural ecosystems have been studied extensively [29,37–40,43–46,49–54,57,60,65,67,68,70,73,75,76,78,80,82–85,87,88]. In contrast, there is only limited knowledge about the diversity and ecological roles of oomycetes in forest canopies, mainly gained from studies of often devastating diseases in temperate oceanic regions associated with (i) invasive aerial *Phytophthora* species like *P. ramorum* causing “Sudden Oak Death” in California and Oregon or “Sudden Larch Death” in the British Isles [43,48,62]; *P. kernoviae* causing aerial bark cankers on *Fagus sylvatica* in the UK [128]; *P. pinifolia* causing shoot and needle blight and defoliations of *Pinus radiata*



in Chile [59]; *P. pluvialis* causing red needle cast of *P. radiata* in New Zealand [129] and branch and stem cankers and defoliations of *Tsuga heterophylla* in the UK [66]; or (ii) native aerial *Phytophthora* species like *P. pseudosyringae* causing bark cankers and dieback of exotic *Nothofagus* species in the UK [69]; *P. nemorosa* and *P. siskiyouensis* causing scattered bark cankers on *Notholithocarpus densiflorus* and other tree species in the Pacific Northwest [47]; and *P. ilicis* causing leaf, shoot and fruit blight on the native *Ilex aquifolium* in Sardinia, Italy [130]. Isolations from necrotic lesions of naturally fallen tree leaves indicate that in their centres of origin, *P. ramorum* (laurosilva forests in Vietnam and Japan); *P. kernoviae* and *P. pseudokernoviae* (Valdivian rainforests in Chile); and *P. celebensis*, *P. javanensis* and *P. multiglobulosa* (tropical rainforests in Indonesia) thrive in forest canopies as benign seasonal colonisers of senescent leaves [31,44,45,131,132]. Numerous leaf, shoot and fruit blights and canker diseases caused by aerial *Phytophthora* pathogens, including *P. botryosa*, *P. capsici*, *P. heterospora*, *P. meadii*, *P. megakarya*, *P. palmivora* and *P. tropicalis*, on tropical tree crops [8,26,133–142] and the findings of *S. medusiformis* on naturally fallen tree leaves and stem tissue in tropical cloud forests in Panama and Ecuador predict a rich community of aerial *Phytophthoras* and other oomycetes inhabiting tropical forest canopies. Extensive surveys in canopies of tropical lowland and montane forests using both isolation tests and metagenomic approaches from necrotic leaf, shoot, fruit and bark tissues, canopy-drip samples and spore traps are needed in both wet and dry seasons to unveil the diversity of tropical aerial oomycetes and their ecological roles and host associations.

The morphological and physiological attributes of *P. parvispora* provide insights into the ecology and survival strategy of this pathogen. Having high cardinal temperatures for growth >12, 27 and 37 °C, respectively, *P. parvispora* is well adapted to tropical and subtropical climates and greenhouse conditions, which is reflected by all known disease outbreaks.

**Supplementary Materials:** The following are available online at <https://www.mdpi.com/article/10.3390/jof9050517/s1>, Table S1: Details of isolates from *Synchrospora* and related oomycete genera considered in the phylogenetic studies.

**Author Contributions:** Conceptualisation, T.J., Y.B. and M.H.J.; methodology, Y.B., M.H.J., T.K. and T.J.; formal analysis, Y.B., T.J., K.D.B., I.M., B.Đ., J.J., T.K. and M.H.J.; investigation, Y.B., T.J., K.D.B., I.M. and M.H.J.; data curation, T.J. and M.H.J.; writing—original draft preparation, T.J. and M.H.J.; writing—review and editing, T.J., M.H.J., Y.B., K.D.B., I.M., J.J., B.Đ. J.J. and T.K.; funding acquisition, T.J. and M.H.J. All authors have read and agreed to the published version of the manuscript.

**Funding:** This study was supported by the Project *Phytophthora* Research Centre Reg. No. CZ.02.1.01/0.0/0.0/15\_003/0000453, financed by the Czech Ministry for Education, Youth and Sports and the European Regional Development Fund.

**Institutional Review Board Statement:** Not applicable.

**Informed Consent Statement:** Not applicable.

**Data Availability Statement:** All sequences generated during this study are available from GenBank, and accession numbers are given in Table S1. All datasets and trees derived from BI and ML analyses are available from DRYAD (<https://datadryad.org>, accessed on 24 April 2023) (Dryad Dataset, <https://doi.org/10.5061/dryad.p2ngf1vvt>).

**Acknowledgments:** We thank Aneta Bačová, Anna Hýsková, Henrieta Ďatková and Milica Raco (all at Mendel University in Brno, Czech Republic) for much appreciated technical support.

**Conflicts of Interest:** The authors declare no conflict of interest.

## References

- Dick, M.W. *Straminipilous fungi: Systematics of the Peronosporomycetes Including Accounts of the Marine Straminipilous Protists, the Plasmodiophorids and Similar Organisms*; Kluwer: Dordrecht, The Netherlands, 2001.
- Hulvey, J.; Telle, S.; Nigrelli, L.; Lamour, K.; Thines, M. Salisapiliaceae—A new family of oomycetes from marsh grass litter of southeastern North America. *Persoonia* **2010**, *25*, 109–116. [[CrossRef](#)] [[PubMed](#)]
- Beakes, G.W.; Honda, T.; Thines, M. Systematics of the Stramenipila: Labyrinthulomycota, Hyphochytridiomycota, and Oomycota. In *Systematics and Evolution*; McLaughlin, D.J., Spatafora, J., Eds.; Springer: New York, NY, USA, 2014; pp. 39–97.

4. Thines, M.; Choi, Y.-J. Evolution, diversity and taxonomy of the Peronosporaceae, with focus on the genus *Peronospora*. *Phytopathology* **2016**, *106*, 6–18. [[CrossRef](#)] [[PubMed](#)]
5. Bennett, R.M.; de Cock, A.W.A.M.; Lévesque, A.; Thines, M. *Calycofera* gen. nov., an estuarine sister taxon to *Phytophthium*, Peronosporaceae. *Mycol. Prog.* **2017**, *16*, 947–954. [[CrossRef](#)]
6. Jung, T.; Scanu, B.; Bakonyi, J.; Seress, D.; Kovács, G.M.; Durán, A.; Sanfuentes von Stowasser, E.; Schena, L.; Mosca, S.; Thu, P.Q.; et al. *Nothophytophthora* gen. nov., a new sister genus of *Phytophthora* from natural and semi-natural ecosystems. *Persoonia* **2017**, *39*, 143–174. [[CrossRef](#)]
7. Bourret, T.B.; Choudhury, R.A.; Mehl, H.K.; Blomquist, C.L.; McRoberts, N.; Rizzo, D.M. Multiple origins of downy mildews and mito-nuclear discordance within the paraphyletic genus *Phytophthora*. *PLoS ONE* **2018**, *13*, e0192502. [[CrossRef](#)]
8. Scanu, B.; Jung, T.; Masigol, H.; Linaldeddu, B.T.; Horta Jung, M.; Brandano, A.; Mostowfizadeh-Ghalamfarsa, R.; Janoušek, J.; Riolo, M.; Cacciola, S.O. *Phytophthora heterospora* sp. nov., a new pseudoconidia-producing sister species of *P. palmivora*. *J. Fungi* **2021**, *7*, 870. [[CrossRef](#)]
9. Maia, C.; Horta Jung, M.; Carella, G.; Milenković, I.; Janoušek, J.; Tomšovský, M.; Mosca, S.; Schena, L.; Cravador, A.; Moricca, S.; et al. Eight new *Halophytophthora* species from marine and brackish-water ecosystems in Portugal and an updated phylogeny for the genus. *Persoonia* **2022**, *48*, 54–90. [[CrossRef](#)]
10. Cooke, D.E.L.; Drenth, A.; Duncan, J.M.; Wagels, G.; Brasier, C.M. A molecular phylogeny of *Phytophthora* and related oomycetes. *Fungal Genet. Biol.* **2000**, *30*, 17–32. [[CrossRef](#)]
11. Riethmüller, A.; Voglmayr, H.; Göker, M.; Weiß, M.; Oberwinkler, F. Phylogenetic relationships of the downy mildews (Peronosporales) and related groups based on nuclear large subunit ribosomal DNA sequences. *Mycologia* **2002**, *94*, 834–849. [[CrossRef](#)]
12. Kroon, L.P.N.M.; Bakker, F.T.; van den Bosch, G.B.M.; Bonants, P.J.M.; Flier, W.G. Phylogenetic analysis of *Phytophthora* species based on mitochondrial and nuclear DNA sequences. *Fungal Genet. Biol.* **2004**, *41*, 766–782. [[CrossRef](#)]
13. Göker, M.; Voglmayr, H.; Riethmüller, A.; Oberwinkler, F. How do obligate parasites evolve? A multi-gene phylogenetic analysis of downy mildews. *Fungal Genet. Biol.* **2007**, *44*, 105–122. [[CrossRef](#)]
14. Runge, F.; Telle, S.; Ploch, S.; Savory, E.; Day, B.; Sharma, R.; Thines, M. The inclusion of downy mildews in a multi-locus-dataset and its reanalysis reveals a high degree of paraphyly in *Phytophthora*. *IMA Fungus* **2011**, *2*, 163–171. [[CrossRef](#)]
15. Martin, F.N.; Blair, J.E.; Coffey, M.D. A combined mitochondrial and nuclear multilocus phylogeny of the genus *Phytophthora*. *Fungal Genet. Biol.* **2014**, *66*, 19–32. [[CrossRef](#)]
16. Brasier, C.; Scanu, B.; Cooke, D.; Jung, T. *Phytophthora*: An ancient, historic, biologically and structurally cohesive and evolutionarily successful generic concept in need of preservation. *IMA Fungus* **2022**, *13*, 12. [[CrossRef](#)]
17. Briard, M.; Dutertre, M.; Rouxel, F.; Brygoo, Y. Ribosomal RNA sequence divergence within the Pythiaceae. *Mycol. Res.* **1995**, *99*, 1119–1127. [[CrossRef](#)]
18. de Cock, A.W.A.M.; Lévesque, C.A. New species of *Pythium* and *Phytophthora*. *Stud. Mycol.* **2004**, *50*, 481–487.
19. Villa, N.O.; Kageyama, K.; Asano, T.; Suga, H. Phylogenetic relationships of *Pythium* and *Phytophthora* species based on ITS rDNA, cytochrome oxidase II and beta-tubulin gene sequences. *Mycologia* **2006**, *98*, 410–422. [[PubMed](#)]
20. Bala, K.; Robideau, G.P.; Lévesque, C.A.; de Cock, A.W.A.M.; Abad, Z.G.; Lodhi, A.M.; Shahzad, S.; Ghaffar, A.; Coffey, M.D. *Phytophthium* *Abad*, *de Cock*, *Bala*, *Robideau*, *Lodhi* & *Lévesque*, gen. nov. and *Phytophthium* *sindhium* *Lodhi*, *Shahzad* & *Lévesque*, sp. nov. *Fungal Planet* **2010**, *24*, 136–137.
21. Uzuhashi, S.; Tojo, M.; Kakishima, M. Phylogeny of the genus *Pythium* and description of new genera. *Mycoscience* **2010**, *51*, 337–365. [[CrossRef](#)]
22. de Cock, A.W.A.M.; Lodhi, A.M.; Rintoul, T.L.; Bala, K.; Robideau, G.P.; Abad, Z.G.; Coffey, M.D.; Shahzad, S.; Lévesque, C.A. *Phytophthium*: Molecular phylogeny and systematics. *Persoonia* **2015**, *34*, 25–39. [[CrossRef](#)]
23. Nguyen, H.D.T.; Dodge, A.; Dadej, K.; Rintoul, T.L.; Ponomareva, E.; Martin, F.N.; de Cock, A.W.A.M.; Lévesque, C.A.; Redhead, S.A.; Spies, C.F.J. Whole genome sequencing and phylogenomic analysis show support for the splitting of genus *Pythium*. *Mycologia* **2022**, *114*, 501–515. [[CrossRef](#)]
24. Gäumann, E.A. *The Fungi. A Description of Their Morphological Features and Evolutionary Development*; Hafner Publishing: New York, NY, USA; London, UK, 1952.
25. Newell, S.Y.; Fell, J.W. Do halophytophthoras (marine Pythiaceae) rapidly occupy fallen leaves by intraleaf mycelial growth? *Can. J. Bot.* **1995**, *73*, 761–765. [[CrossRef](#)]
26. Erwin, D.C.; Ribeiro, O.K. *Phytophthora Diseases Worldwide*; APS Press: St. Paul, MN, USA, 1996.
27. Leaño, E.M.; Jones, E.B.G.; Vrijmoed, L.L.P. Why are *Halophytophthora* species well adapted to mangrove habitats? *Fungal Divers.* **2000**, *5*, 131–151.
28. Nakagiri, A. Ecology and biodiversity of *Halophytophthora* species. *Fungal Divers.* **2000**, *5*, 153–164.
29. Brasier, C.M.; Cooke, D.E.L.; Duncan, J.M.; Hansen, E.M. Multiple new phenotypic taxa from trees and riparian ecosystems in *Phytophthora gonapodyides*-*P. megasperma* ITS Clade 6, which tend to be high-temperature tolerant and either inbreeding or sterile. *Mycol. Res.* **2003**, *107*, 277–290. [[CrossRef](#)]
30. Jung, T.; Stukely, M.J.C.; Hardy, G.E.S.J.; White, D.; Paap, T.; Dunstan, W.A.; Burgess, T.I. Multiple new *Phytophthora* species from ITS Clade 6 associated with natural ecosystems in Australia: Evolutionary and ecological implications. *Persoonia* **2011**, *26*, 13–39. [[CrossRef](#)]

31. Jung, T.; Milenković, I.; Corcobado, T.; Májek, T.; Janoušek, J.; Kudláček, T.; Tomšovský, M.; Nagy, Z.; Durán, A.; Tarigan, M.; et al. Extensive morphological and behavioural diversity among fourteen new and seven described species in Phytophthora Clade 10 and its evolutionary implications. *Persoonia* **2022**, *49*, 1–57. [[CrossRef](#)]
32. Bennett, R.M.; Nam, B.; Dedeles, G.R.; Thines, M. *Phytophthora leanoi* sp. nov. and *Phytophthora dogmae* sp. nov., *Phytophthora* species associated with mangrove leaf litter from the Philippines. *Acta Mycol.* **2017**, *52*, 1103. [[CrossRef](#)]
33. Jesus, A.L.; Marano, A.V.; Gonçalves, D.R.; Jerônimo, G.H.; Pires-Zottarelli, C.L.A. Two new species of *Halophytophthora* from Brazil. *Mycol. Prog.* **2019**, *18*, 1411–1421. [[CrossRef](#)]
34. Chen, Q.; Bakhshi, M.; Balci, Y.; Broders, K.D.; Cheewangkoon, R.; Chen, S.F.; Fan, X.L.; Gramaje, D.; Halleen, F.; Horta Jung, M.; et al. Genera of phytopathogenic fungi: GOPHY 4. *Stud. Mycol.* **2022**, *101*, 417–564. [[CrossRef](#)]
35. Beakes, G.W.; Glockling, S.L.; Sekimoto, S. The evolutionary phylogeny of the oomycete “fungi”. *Protoplasma* **2012**, *249*, 3–19. [[CrossRef](#)] [[PubMed](#)]
36. O’Hanlon, R.; Destefanis, M.; Milenković, I.; Tomšovský, M.; Janoušek, J.; Bellgard, S.E.; Weir, B.S.; Kudláček, T.; Horta Jung, M.; Jung, T. Two new *Nothophytophthora* species from streams in Ireland and Northern Ireland: *Nothophytophthora irlandica* and *N. lirii* sp. nov. *PLoS ONE* **2021**, *16*, e0250527. [[CrossRef](#)] [[PubMed](#)]
37. Brasier, C.M.; Robredo, F.; Ferraz, J.F.P. Evidence for *Phytophthora cinnamomi* involvement in Iberian oak decline. *Plant Pathol.* **1993**, *42*, 140–145. [[CrossRef](#)]
38. Brasier, C.M.; Kirk, S.A.; Delcan, J.; Cooke, D.E.L.; Jung, T.; In’T Veld, W.A.M. *Phytophthora alni* sp. nov. and its variants: Designation of emerging heteroploid hybrid pathogens spreading on *Alnus* trees. *Mycol. Res.* **2004**, *108*, 1172–1184. [[CrossRef](#)]
39. Jung, T.; Blaschke, H.; Neumann, P. Isolation, identification and pathogenicity of *Phytophthora* species from declining oak stands. *Eur. J. For. Pathol.* **1996**, *26*, 253–272. [[CrossRef](#)]
40. Jung, T.; Blaschke, H.; Osswald, W. Involvement of soilborne *Phytophthora* species in Central European oak decline and the effect of site factors on the disease. *Plant Pathol.* **2000**, *49*, 706–718. [[CrossRef](#)]
41. Jung, T.; Vettraino, A.M.; Cech, T.L.; Vannini, A. The impact of invasive *Phytophthora* species on European forests. In *Phytophthora: A Global Perspective*; Lamour, K., Ed.; CABI: Wallingford, UK, 2013; pp. 146–158.
42. Jung, T.; Orlikowski, L.; Henricot, B.; Abad-Campos, P.; Aday, A.G.; Aguin Casal, O.; Bakonyi, J.; Cacciola, S.O.; Cech, T.; Chavarriaga, D.; et al. Widespread *Phytophthora* infestations in European nurseries put forest, semi-natural and horticultural ecosystems at high risk of *Phytophthora* diseases. *For. Pathol.* **2016**, *46*, 134–163. [[CrossRef](#)]
43. Jung, T.; Pérez-Sierra, A.; Durán, A.; Horta Jung, M.; Balci, Y.; Scanu, B. Canker and decline diseases caused by soil- and airborne *Phytophthora* species in forests and woodlands. *Persoonia* **2018**, *40*, 182–220. [[CrossRef](#)]
44. Jung, T.; Durán, A.; von Stowasser, E.S.; Schena, L.; Mosca, S.; Fajardo, S.; González, M.; Navarro Ortega, A.D.; Bakonyi, J.; Seress, D.; et al. Diversity of *Phytophthora* species in Valdivian rainforests and association with severe dieback symptoms. *For. Pathol.* **2018**, *48*, e12443. [[CrossRef](#)]
45. Jung, T.; Scanu, B.; Brasier, C.M.; Webber, J.; Milenković, I.; Corcobado, T.; Tomšovský, T.; Pánek, M.; Bakonyi, J.; Maia, C.; et al. A survey in natural forest ecosystems of Vietnam reveals high diversity of both new and described *Phytophthora* taxa including *P. ramorum*. *Forests* **2020**, *11*, 93. [[CrossRef](#)]
46. Hansen, E.M.; Goheen, D.J.; Jules, E.S.; Ullian, B. Managing Port–Orford–Cedar and the introduced pathogen *Phytophthora lateralis*. *Plant Dis.* **2000**, *84*, 4–14. [[CrossRef](#)]
47. Hansen, E.M.; Reeser, P.W.; Sutton, W. *Phytophthora* beyond agriculture. *Annu. Rev. Phytopathol.* **2012**, *50*, 359–378. [[CrossRef](#)]
48. Rizzo, D.M.; Garbelotto, M.; Davidson, J.M.; Slaughter, G.W.; Koike, S.T. *Phytophthora ramorum* as the cause of extensive mortality of *Quercus* spp. and *Lithocarpus densiflorus* in California. *Plant Dis.* **2002**, *86*, 205–214. [[CrossRef](#)]
49. Vettraino, A.M.; Barzanti, G.P.; Bianco, M.C.; Ragazzi, A.; Capretti, P.; Paoletti, E.; Luisi, N.; Anselmi, N.; Vannini, A. Occurrence of *Phytophthora* species in oak stands in Italy and their association with declining oak trees. *For. Pathol.* **2002**, *32*, 19–28. [[CrossRef](#)]
50. Vettraino, A.M.; Morel, O.; Perlerou, C.; Robin, C.; Diamandis, S.; Vannini, A. Occurrence and distribution of *Phytophthora* species associated with Ink Disease of chestnut in Europe. *Eur. J. Plant Pathol.* **2005**, *111*, 169–180. [[CrossRef](#)]
51. Balci, Y.; Halmschlager, E. Incidence of *Phytophthora* species in oak forests in Austria and their possible involvement in oak decline. *For. Pathol.* **2003**, *33*, 157–174. [[CrossRef](#)]
52. Balci, Y.; Halmschlager, E. *Phytophthora* species in oak ecosystems in Turkey and their association with declining oak trees. *Plant Pathol.* **2003**, *52*, 694–702. [[CrossRef](#)]
53. Jönsson, U.; Lundberg, L.; Sonesson, K.; Jung, T. First records of soilborne *Phytophthora* species in Swedish oak forests. *For. Pathol.* **2003**, *33*, 175–179. [[CrossRef](#)]
54. Jung, T.; Blaschke, M. *Phytophthora* root and collar rot of alders in Bavaria: Distribution, modes of spread and possible management strategies. *Plant Pathol.* **2004**, *53*, 197–208. [[CrossRef](#)]
55. Hardham, A.R. *Phytophthora cinnamomi*. *Mol. Plant Pathol.* **2005**, *6*, 589–604. [[CrossRef](#)]
56. Balci, Y.; Balci, S.; Eggers, J.; MacDonald, W.L.; Juzwik, J.; Long, R.P.; Gottschalk, K.W. *Phytophthora* spp. associated with forest soils in Eastern and North–Central U.S. oak ecosystems. *Plant Dis.* **2007**, *91*, 705–710. [[CrossRef](#)] [[PubMed](#)]
57. Balci, Y.; Long, R.P.; Mansfield, M.; Balser, D.; MacDonald, W.L. Involvement of *Phytophthora* species in white oak (*Quercus alba*) decline in southern Ohio. *For. Pathol.* **2010**, *40*, 430–442. [[CrossRef](#)]
58. Greslebin, A.; Hansen, E.M.; Sutton, W. *Phytophthora austrocedrae* sp. nov., a new species associated with *Austrocedrus chilensis* mortality in Patagonia (Argentina). *Mycol. Res.* **2007**, *111*, 308–316. [[CrossRef](#)] [[PubMed](#)]

59. Durán, A.; Gryzenhout, M.; Slippers, B.; Ahumada, R.; Rotella, A.; Flores, F.; Wingfield, B.D.; Wingfield, M.J. *Phytophthora pinifolia* sp. nov. associated with a serious needle disease of *Pinus radiata* in Chile. *Plant Pathol.* **2008**, *57*, 715–727. [[CrossRef](#)]
60. Jung, T. Beech decline in Central Europe driven by the interaction between *Phytophthora* infections and climatic extremes. *For. Pathol.* **2009**, *39*, 73–94. [[CrossRef](#)]
61. Jung, T.; Burgess, T.I. Re-evaluation of *Phytophthora citricola* isolates from multiple woody hosts in Europe and North America reveals a new species, *Phytophthora plurivora* sp. nov. *Persoonia* **2009**, *22*, 95–110. [[CrossRef](#)]
62. Brasier, C.; Webber, J. Sudden larch death. *Nature* **2010**, *466*, 824–825. [[CrossRef](#)]
63. Green, S.; Brasier, C.M.; Schlenzig, A.; McCracken, A.; MacAskill, G.A.; Wilson, M.; Webber, J.F. The destructive invasive pathogen *Phytophthora lateralis* found on *Chamaecyparis lawsoniana* across the UK. *For. Pathol.* **2013**, *43*, 19–28.
64. Green, S.; Elliot, M.; Armstrong, A.; Hendry, S.J. *Phytophthora austrocedrae* emerges as a serious threat to juniper (*Juniperus communis*) in Britain. *Plant Pathol.* **2015**, *64*, 456–466. [[CrossRef](#)]
65. Pérez-Sierra, A.; López-García, C.; León, M.; García-Jiménez, J.; Abad-Campos, P.; Jung, T. Previously unrecorded low temperature *Phytophthora* species associated with *Quercus* decline in a Mediterranean forest in Eastern Spain. *For. Pathol.* **2013**, *43*, 331–339. [[CrossRef](#)]
66. Pérez-Sierra, A.; Chitty, R.; Eacock, A.; Jones, B.; Biddle, M.; Crampton, M.; Lewis, A.; Olivieri, L.; Webber, J.F. First report of *Phytophthora pluvialis* in Europe causing resinous cankers on western hemlock. *New Dis. Rep.* **2022**, *45*, e12064. [[CrossRef](#)]
67. Ginetti, B.; Moricca, S.; Squires, J.N.; Cooke, D.E.L.; Ragazzi, A.; Jung, T. *Phytophthora acerina* sp. nov., a new species causing bleeding cankers and dieback of *Acer pseudoplatanus* trees in planted forests in Northern Italy. *Plant Pathol.* **2014**, *63*, 858–876. [[CrossRef](#)]
68. Scanu, B.; Linaldeddu, B.T.; Deidda, A.; Jung, T. Diversity of *Phytophthora* species from declining Mediterranean maquis vegetation, including two new species, *Phytophthora crassamura* and *P. ornamentata* sp. nov. *PLoS ONE* **2015**, *10*, e0143234. [[CrossRef](#)]
69. Scanu, B.; Webber, J.F. Dieback and mortality of *Nothofagus* in Britain: Ecology, pathogenicity and sporulation potential of the causal agent *Phytophthora pseudosyringae*. *Plant Pathol.* **2016**, *65*, 26–36. [[CrossRef](#)]
70. Milenković, I.; Keča, N.; Karadžić, D.; Radulović, Z.; Nowakowska, J.A.; Oszako, T.; Sikora, K.; Corcobado, T.; Jung, T. Isolation and pathogenicity of *Phytophthora* species from poplar plantations in Serbia. *Forests* **2018**, *9*, 330. [[CrossRef](#)]
71. Corcobado, T.; Cech, T.L.; Brandstetter, M.; Daxer, A.; Hüttler, C.; Kudláček, T.; Horta Jung, M.; Jung, T. Decline of European beech in Austria: Involvement of *Phytophthora* spp. and contributing biotic and abiotic factors. *Forests* **2020**, *11*, 895. [[CrossRef](#)]
72. Jung, T.; Hansen, E.M.; Winton, L.; Oßwald, W.; Delatour, C. Three new species of *Phytophthora* from European oak forests. *Mycol. Res.* **2002**, *106*, 397–411. [[CrossRef](#)]
73. Jung, T.; Chang, T.T.; Bakonyi, J.; Seress, D.; Pérez-Sierra, A.; Yang, X.; Hong, C.; Scanu, B.; Fu, C.H.; Hsueh, K.-L.; et al. Diversity of *Phytophthora* species in natural ecosystems of Taiwan and association with disease symptoms. *Plant Pathol.* **2017**, *66*, 194–211. [[CrossRef](#)]
74. Jung, T.; Horta Jung, M.; Scanu, B.; Seress, D.; Kovács, D.M.; Maia, C.; Pérez-Sierra, A.; Chang, T.-T.; Chandelier, A.; Heungens, A.; et al. Six new *Phytophthora* species from ITS Clade 7a including two sexually functional heterothallic hybrid species detected in natural ecosystems in Taiwan. *Persoonia* **2017**, *38*, 100–135. [[CrossRef](#)]
75. Jung, T.; Horta Jung, M.; Cacciola, S.O.; Cech, T.; Bakonyi, J.; Seress, D.; Mosca, S.; Schena, L.; Seddaiu, S.; Pane, A.; et al. Multiple new cryptic pathogenic *Phytophthora* species from Fagaceae forests in Austria, Italy and Portugal. *IMA Fungus* **2017**, *8*, 219–244. [[CrossRef](#)]
76. Jung, T.; La Spada, F.; Pane, A.; Aloï, F.; Evoli, M.; Horta Jung, M.; Scanu, B.; Faedda, R.; Rizza, C.; Puglisi, I.; et al. Diversity and distribution of *Phytophthora* species in protected natural areas in Sicily. *Forests* **2019**, *10*, 259. [[CrossRef](#)]
77. Zeng, H.-C.; Ho, H.-H.; Zheng, F.-C. A survey of *Phytophthora* species on Hainan Island of South China. *J. Phytopathol.* **2009**, *157*, 33–39. [[CrossRef](#)]
78. Brasier, C.M.; Vettraino, A.M.; Chang, T.T.; Vannini, A. *Phytophthora lateralis* discovered in an old growth *Chamaecyparis* forest in Taiwan. *Plant Pathol.* **2010**, *59*, 595–603. [[CrossRef](#)]
79. Rea, A.J.; Burgess, T.I.; Hardy, G.E.S.J.; Stukely, M.J.C.; Jung, T. Two novel and potentially endemic species of *Phytophthora* associated with episodic dieback of kwongan vegetation in the south-west of Western Australia. *Plant Pathol.* **2011**, *60*, 1055–1068. [[CrossRef](#)]
80. Reeser, P.W.; Sutton, W.; Hansen, E.M.; Remigi, P.; Adams, G.C. *Phytophthora* species in forest streams in Oregon and Alaska. *Mycologia* **2011**, *103*, 22–35. [[CrossRef](#)]
81. Vettraino, A.M.; Brasier, C.M.; Brown, A.V.; Vannini, A. *Phytophthora himalsilva* sp. nov. an unusually phenotypically variable species from a remote forest in Nepal. *Fungal Biol.* **2011**, *115*, 275–287. [[CrossRef](#)]
82. Huai, W.X.; Tian, G.; Hansen, E.M.; Zhao, W.-X.; Goheen, E.M.; Grünwald, N.J.; Cheng, C. Identification of *Phytophthora* species baited and isolated from forest soil and streams in northwestern Yunnan province, China. *For. Pathol.* **2013**, *43*, 87–103. [[CrossRef](#)]
83. Huberli, D.; Hardy, G.E.S.J.; White, D.; Williams, N.; Burgess, T.I. Fishing for *Phytophthora* from Western Australia's waterways: A distribution and diversity survey. *Australas. Plant Pathol.* **2013**, *42*, 251–260. [[CrossRef](#)]
84. Oh, E.; Gryzenhout, M.; Wingfield, B.D.; Wingfield, M.J.; Burgess, T.I. Surveys of soil and water reveal a goldmine of *Phytophthora* diversity in South African natural ecosystems. *IMA Fungus* **2013**, *4*, 123–131. [[CrossRef](#)]

85. Shrestha, S.K.; Zhou, Y.; Lamour, K. Oomycetes baited from streams in Tennessee 2010–2012. *Mycologia* **2013**, *105*, 1516–1523. [[CrossRef](#)]
86. Català, S.; Pérez-Sierra, A.; Abad-Campos, P. The use of genus-specific amplicon pyrosequencing to assess Phytophthora species diversity using eDNA from soil and water in Northern Spain. *PLoS ONE* **2015**, *10*, e0119311. [[CrossRef](#)]
87. Brazeel, N.J.; Wick, R.L.; Hulvey, J.P. Phytophthora species recovered from the Connecticut River Valley in Massachusetts, USA. *Mycologia* **2016**, *108*, 6–19. [[CrossRef](#)]
88. Dunstan, W.A.; Howard, K.; Hardy, G.E.S.J.; Burgess, T.I. An overview of Australia's Phytophthora species assemblage in natural ecosystems recovered from a survey in Victoria. *IMA Fungus* **2016**, *7*, 47–58. [[CrossRef](#)]
89. O'Hanlon, R.; Choiseul, J.; Corrigan, M.; Catarama, T.; Destefanis, M. Diversity and detections of Phytophthora species from trade and nontrade environments in Ireland. *Bull. OEPP* **2016**, *46*, 594–602. [[CrossRef](#)]
90. Burgess, T.I.; White, D.; McDougall, K.M.; Garnas, J.; Dunstan, W.A.; Català, S.; Carnegie, A.J.; Worboys, S.; Cahill, D.; Vettraino, A.-M.; et al. Distribution and diversity of Phytophthora across Australia. *Pac. Conserv. Biol.* **2017**, *23*, 1–13. [[CrossRef](#)]
91. Burgess, T.I.; Simamora, A.V.; White, D.; Williams, B.; Schwager, M.; Stukely, M.J.C.; Hardy, G.E.S.J. New species from Phytophthora Clade 6a: Evidence for recent radiation. *Persoonia* **2018**, *41*, 1–17. [[CrossRef](#)]
92. Burgess, T.I.; Dang, Q.N.; Le, B.V.; Pham, N.Q.; White, D.; Pham, T.Q. Phytophthora acaciivora sp. nov. associated with dying Acacia mangium in Vietnam. *FUSE* **2020**, *6*, 243–252. [[CrossRef](#)]
93. Bose, T.; Hulbert, J.M.; Burgess, T.I.; Paap, T.; Roets, F.; Wingfield, M.J. Two novel Phytophthora species from the southern tip of Africa. *Mycol. Prog.* **2021**, *20*, 755–767. [[CrossRef](#)]
94. Dang, Q.N.; Pham, T.Q.; Arentz, F.; Hardy, G.E.S.J.; Burgess, T.I. New Phytophthora species in clade 2a from the Asia-Pacific region including a re-examination of P. colocasiae and P. meadii. *Mycol. Prog.* **2021**, *20*, 111–129. [[CrossRef](#)]
95. Katoh, K.; Standley, D.M. MAFFT multiple sequence alignment software version 7: Improvements in performance and usability. *Mol. Biol. Evol.* **2013**, *30*, 772–780. [[CrossRef](#)]
96. Lanfear, R.; Frandsen, P.; Wright, A.; Senfeld, T.; Calcott, B. PartitionFinder 2: New methods for selecting partitioned models of evolution for molecular and morphological phylogenetic analyses. *Mol. Biol. Evol.* **2016**, *34*, 772–773. [[CrossRef](#)] [[PubMed](#)]
97. Kozlov, A.; Darriba, D.; Flouri, T.; Morel, B.; Stamatakis, A. RAxML-NG: A fast, scalable and user-friendly tool for maximum likelihood phylogenetic inference. *Bioinformatics* **2019**, *35*, 4453–4455. [[CrossRef](#)] [[PubMed](#)]
98. Pattengale, N.; Alipour, M.; Bininda-Emonds, O.; Moret, B.; Stamatakis, A. How many bootstrap replicates are necessary? *J. Comput. Biol.* **2010**, *17*, 337–354. [[CrossRef](#)] [[PubMed](#)]
99. Lemoine, F.; Domelevo Entfellner, J.; Wilkinson, E.; Correia, D.; Dávila Felipe, M.; De Oliveira, T.; Gascuel, O. Renewing Felsenstein's phylogenetic bootstrap in the era of big data. *Nature* **2018**, *556*, 452–456. [[CrossRef](#)]
100. Sukumaran, J.; Holder, M.T. DendroPy: A Python library for phylogenetic computing. *Bioinformatics* **2010**, *26*, 1569–1571. [[CrossRef](#)]
101. Müller, N.; Bouckaert, R. Adaptive parallel tempering for BEAST 2. *bioRxiv* **2019**, 603514. [[CrossRef](#)]
102. Kone, A.; Kofke, D.A. Selection of temperature intervals for parallel-tempering simulations. *J. Chem. Phys.* **2005**, *122*, 1–2. [[CrossRef](#)]
103. Atchadé, Y.F.; Roberts, G.O.; Rosenthal, J.S. Towards optimal scaling of metropolis-coupled Markov chain Monte Carlo. *Stat. Comput.* **2011**, *21*, 555–568. [[CrossRef](#)]
104. Bouckaert, R.; Drummond, A. bModelTest: Bayesian phylogenetic site model averaging and model comparison. *BMC Evol. Biol.* **2017**, *17*, 42. [[CrossRef](#)]
105. Drummond, A.J.; Ho, S.Y.W.; Phillips, M.J.; Rambaut, A. Relaxed phylogenetics and dating with confidence. *PLoS Biol.* **2006**, *4*, 699–710. [[CrossRef](#)]
106. Rambaut, A.; Drummond, A.; Xie, D.; Baele, G.; Suchard, M. Posterior summarization in Bayesian phylogenetics using Tracer 1.7. *Syst. Biol.* **2018**, *67*, 901–904. [[CrossRef](#)]
107. Stöver, B.C.; Müller, K.F. TreeGraph 2: Combining and visualizing evidence from different phylogenetic analyses. *BMC Bioinform.* **2010**, *11*, 7. [[CrossRef](#)]
108. Tamura, K.; Stecher, G.; Kumar, S. MEGA11: Molecular Evolutionary Genetics Analysis version 11. *Mol. Biol. Evol.* **2021**, *38*, 3022–3027. [[CrossRef](#)]
109. Blair, J.E.; Coffey, M.D.; Park, S.-Y.; Greiser, D.M.; Kang, S. A multi-locus phylogeny for Phytophthora utilizing markers derived from complete genome sequences. *Fungal Genet. Biol.* **2008**, *45*, 266–277. [[CrossRef](#)]
110. Robideau, G.P.; de Cock, A.W.A.M.; Coffey, M.D.; Voglmayr, H.; Brouwer, H.; Bala, K.; Chitty, D.W.; Désaulniers, N.; Eggertson, Q.A.; Gachon, C.M.M.; et al. DNA barcoding of oomycetes with cytochrome c oxidase subunit I and internal transcribed spacer. *Mol. Ecol. Resour.* **2011**, *11*, 1002–1011. [[CrossRef](#)]
111. Martin, F.N. Phylogenetic relationships among some Pythium species inferred from sequence analysis of the mitochondrially encoded cytochrome oxidase II gene. *Mycologia* **2000**, *92*, 711–727. [[CrossRef](#)]
112. Martin, F.N.; Tooley, P.W. Phylogenetic relationships among Phytophthora species inferred from sequence analysis of mitochondrially encoded cytochrome oxidase I and II genes. *Mycologia* **2003**, *95*, 269–284. [[CrossRef](#)]
113. Hudspeth, D.S.S.; Nadler, S.A.; Hudspeth, M.E.S. A COX2 molecular phylogeny of the Peronosporomycetes. *Mycologia* **2000**, *92*, 674–684. [[CrossRef](#)]

114. White, T.J.; Bruns, T.; Lee, S.; Taylor, J. Amplification and direct sequencing of fungal ribosomal RNA genes for phylogenetics. In *PCR Protocols: A Guide to Methods and Applications*; Innis, M.A., Gelfand, D.H., Sninsky, J.J., White, T.J., Eds.; Academic Press: San Diego, CA, USA, 1990; pp. 315–322.
115. Garbelotto, M.M.; Lee, H.K.; Slaughter, G.; Popenuck, T.; Cobb, F.W.; Brunset, T.D. Heterokaryosis is not required for virulence of *Heterobasidion annosum*. *Mycologia* **1997**, *89*, 92–102. [[CrossRef](#)]
116. Hopple, J.S.; Vilgalys, R. Phylogenetic relationships among coprinoid taxa and allies based on data from restriction site mapping of nuclear rDNA. *Mycologia* **1994**, *86*, 96–107. [[CrossRef](#)]
117. Dick, M.W. *Keys to Pythium*; University of Reading Press: Reading, UK, 1990.
118. Jung, T.; Cooke, D.E.L.; Blaschke, H.; Duncan, J.M.; Oßwald, W. *Phytophthora quercina* sp. nov., causing root rot of European oaks. *Mycol. Res.* **1999**, *103*, 785–798. [[CrossRef](#)]
119. Thines, M. Bridging the Gulf: *Phytophthora* and downy mildews are connected by rare grass parasites. *PLoS ONE* **2009**, *4*, e4790. [[CrossRef](#)] [[PubMed](#)]
120. Barreto, R.W.; Dick, M.W. Monograph of Basidiophora (Oomycetes) with the description of a new species. *Bot. J. Linn. Soc.* **1991**, *107*, 313–332. [[CrossRef](#)]
121. Telle, S.; Thines, M. Reclassification of an enigmatic downy mildew species on lovegrass (*Eragrostis*) to the new genus *Eraphthora*, with a key to the genera of the Peronosporaceae. *Mycol. Prog.* **2012**, *11*, 121–129. [[CrossRef](#)]
122. Thines, M.; Telle, S.; Choi, Y.-J.; Tan, Y.P.; Shivas, R.G. *Baobabopsis*, a new genus of graminicolous downy mildews from tropical Australia, with an updated key to the genera of downy mildews. *IMA Fungus* **2015**, *6*, 483–491. [[CrossRef](#)]
123. Crouch, J.A.; Davis, W.J.; Shishkoff, N.; Castroagudín, V.L.; Martin, F.; Michelmore, R.; Thines, M. Peronosporaceae species causing downy mildew diseases of Poaceae, including nomenclature revisions and diagnostic resources. *FUSE* **2022**, *9*, 43–86. [[CrossRef](#)]
124. Baxter, L.; Tripathy, S.; Ishaque, L.; Boot, N.; Cabral, A.; Kemen, E.; Thines, M.; Ah-Fong, A.; Anderson, R.; Badejoko, W.; et al. Signatures of adaptation to obligate biotrophy in the *Hyaloperonospora arabidopsis* genome. *Science* **2010**, *330*, 1549–1551. [[CrossRef](#)]
125. Falloon, R.E.; Sutherland, P.W. *Peronospora viciae* on *Pisum sativum*: Morphology of asexual and sexual reproductive structures. *Mycologia* **1996**, *88*, 473–483. [[CrossRef](#)]
126. Nordskog, B.; Gadoury, D.M.; Seem, R.C.; Hermansen, A. Impact of diurnal periodicity, temperature, and light on sporulation of *Bremia lactucae*. *Phytopathology* **2007**, *97*, 979–986. [[CrossRef](#)]
127. Kandel, S.L.; Mou, B.; Shishkoff, N.; Shi, A.; Subbarao, K.V.; Klosterman, S.J. Spinach downy mildew: Advances in our understanding of the disease cycle and prospects for disease management. *Plant Dis.* **2019**, *103*, 791–803. [[CrossRef](#)]
128. Brown, A.V.; Brasier, C.M. Colonization of tree xylem by *Phytophthora ramorum*, *P. kernoviae* and other *Phytophthora* species. *Plant Pathol.* **2007**, *56*, 227–241. [[CrossRef](#)]
129. Dick, M.A.; Williams, N.M.; Bader, M.K.-F.; Gardner, J.F.; Bulman, L.S. Pathogenicity of *Phytophthora pluvialis* to *Pinus radiata* and its relation with red needle cast disease in New Zealand. *N. Z. J. For. Sci.* **2014**, *44*, 6. [[CrossRef](#)]
130. Scanu, B.; Linaldeddu, B.T.; Pérez-Sierra, A.; Deidda, A.; Franceschini, A. *Phytophthora ilicis* as a leaf and stem pathogen of *Ilex aquifolium* in Mediterranean islands. *Phytopathol. Mediterr.* **2014**, *53*, 480–490.
131. Sanfuentes, E.; Fajardo, S.; Sabag, M.; Hansen, E.; González, M. *Phytophthora kernoviae* isolated from fallen leaves of *Drymis winteri* in native forest of southern Chile. *Australas. Plant Dis. Notes* **2016**, *11*, 19. [[CrossRef](#)]
132. Jung, T.; Horta Jung, M.; Webber, J.F.; Kageyama, K.; Hieno, A.; Masuya, H.; Uematsu, S.; Pérez-Sierra, A.; Harris, A.R.; Forster, J.; et al. The destructive tree pathogen *Phytophthora ramorum* originates from the Laurosilva forests of East Asia. *J. Fungi* **2021**, *7*, 226. [[CrossRef](#)]
133. Brasier, C.M.; Griffin, M.J. Taxonomy of *Phytophthora palmivora* on cocoa. *Trans. Br. Mycol. Soc.* **1979**, *71*, 111–143. [[CrossRef](#)]
134. Rajalakshmy, V.K.; Joseph, A.; Arthassery, S. Occurrence of two mating groups in *Phytophthora meadii* causing abnormal leaf fall disease of rubber in South India. *Trans. Br. Mycol. Soc.* **1985**, *85*, 723–725. [[CrossRef](#)]
135. Drenth, A.; Guest, D.I. *Diversity and Management of Phytophthora in Southeast Asia*; Australian Centre for International Agricultural Research: Canberra, Australia, 2004.
136. Cerqueira, A.O.; Luz, E.D.M.N.; De Souza, J.T. First record of *Phytophthora tropicalis* causing leaf blight and fruit rot on breadfruit in Brazil. *Plant Pathol.* **2006**, *55*, 296. [[CrossRef](#)]
137. Guest, D.I. Black pod: Diverse pathogens with a global impact on cocoa yield. *Phytopathology* **2007**, *97*, 1650–1653. [[CrossRef](#)]
138. Akrofi, A.Y.; Amoako-Atta, I.; Assuah, M.; Asare, E.K. Black pod disease on cacao (*Theobroma cacao*, L) in Ghana: Spread of *Phytophthora megakarya* and role of economic plants in the disease epidemiology. *Crop Prot.* **2015**, *72*, 66–75. [[CrossRef](#)]
139. Tri, M.V.; Van Hoa, N.; Minh Chau, N.; Pane, A.; Faedda, R.; De Patrizio, A.; Schena, L.; Olsson, C.H.B.; Wright, S.A.I.; Ramstedt, M.; et al. Decline of jackfruit (*Artocarpus heterophyllus*) incited by *Phytophthora palmivora* in Vietnam. *Phytopathol. Mediterr.* **2015**, *54*, 275–280.
140. Puglisi, I.; De Patrizio, A.; Schena, L.; Jung, T.; Evoli, M.; Pane, A.; Hoa, N.V.; Tri, M.V.; Wright, S.; Ramstedt, M.; et al. Two previously unknown *Phytophthora* species associated with brown rot of Pomelo (*Citrus grandis*) fruits in Vietnam. *PLoS ONE* **2017**, *12*, e0172085. [[CrossRef](#)] [[PubMed](#)]

141. Chávez-Ramírez, B.; Rodríguez-Velázquez, N.D.; Chávez-Sánchez, M.E.; Vásquez-Murrieta, M.S.; Hernández-Gallegos, M.A.; Velázquez-Martínez, J.R.; Avendaño-Arrazate, C.H.; Estrada-de los Santos, P. Morphological and molecular identification of *Phytophthora tropicalis* causing black pod rot in Mexico. *Can. J. Plant Pathol.* **2021**, *43*, 670–679. [[CrossRef](#)]
142. Patil, B.; Hedge, V.; Sridhara, S.; Pandian, R.T.P.; Thube, S.H.; Palliath, G.K.; Gangurde, S.S.; Jha, P.K. Multigene phylogeny and haplotype analysis reveals predominance of oomycetous fungus, *Phytophthora meadii* (McRae) associated with fruit rot disease of arecanut in India. *Saudi J. Biol. Sci.* **2019**, *29*, 103341. [[CrossRef](#)]

**Disclaimer/Publisher’s Note:** The statements, opinions and data contained in all publications are solely those of the individual author(s) and contributor(s) and not of MDPI and/or the editor(s). MDPI and/or the editor(s) disclaim responsibility for any injury to people or property resulting from any ideas, methods, instructions or products referred to in the content.